REGULATION OF C4 PHOTOSYNTHETIC DIFFERENTIATION IN *ZEA MAYS*

A Dissertation

Presented to the Faculty of the Graduate School

of Cornell University

In Partial Fulfillment of the Requirements for the Degree of

Doctor of Philosophy

by

Sarah Covshoff

May 2008

REGULATION OF C_4 PHOTOSYNTHETIC DIFFERENTIATION IN *ZEA MAYS*

Sarah Covshoff, Ph. D.

Cornell University 2008

In *Zea mays* (maize), photosynthetic activities are partitioned between two morphologically and biochemically distinct cell types, mesophyll (M) and bundle sheath (BS). These cells are organized as concentric files around the vasculature and functionally cooperate in fixing carbon for photosynthesis. Partitioning of photosynthetic activities between M and BS cells is mediated by cell-specific localization of transcripts and proteins. However, regulation of this process is poorly understood. Here, we utilize two mutants, *hcf136* and *bsd2,* which are selectively disrupted in M or BS cell development, respectively, to dissect the relative importance of sugar, energy metabolites and photosystem II protein complex formation in establishing functional M and BS transcriptional networks. RNA transcript profiling was performed on isolated M and BS cells of WT and mutant siblings, followed by comparative analysis between the two mutants. The results suggest that M and BS transcripts are autonomously regulated by different signals.

BIOGRAPHICAL SKETCH

Sarah Covshoff was born and raised in Toronto, Ontario, Canada. She attended the University of Guelph for her undergraduate degree and received a Bachelors of Science in Agriculture with Distinction in 2002. Upon graduation, Sarah was awarded a two-year Natural Sciences and Engineering Research Council Scholarship, Canada's highest award for academic and research excellence. This award was renewed for another two-year term in the fall of 2004.

During her time at Guelph, Sarah's scientific interests became focused on C_4 photosynthetic biology, and this fascination grew into her research project as a graduate student in Plant Biology at Cornell University in the lab of Dr. Thomas Brutnell. In addition to her research, Sarah was also an active participant in the Postgraduate Society of the BTI. She held the positions of Science Retreat Coordinator for one year and Career Perspectives Series Coordinator for two years. In addition, Sarah was the Teaching Assistant to the Plant Genome Research Outreach Program housed at the BTI, and in that capacity worked with 14 high school science teachers to create seven in-classroom plant molecular biology activities over the course of two years. Sarah also taught and mentored undergraduate students enrolled at Cornell University and a high school student summer intern as part of her lab activities.

I dedicate this dissertation to my family and friends for their enduring support during my time at Cornell. I am most grateful to my parents, Margaret and Philip Covshoff, for their words of wisdom and to my sister, Elana, for her support. I also want to thank Dr. Katia Wostrikoff and Dr. Melanie Sacco for our many inspiring discussions and encouragement throughout this process. As well, I thank my friends who have buoyed my spirits and helped make Ithaca my home away from home.

ACKNOWLEDGMENTS

I would like to thank my advisor Dr. Thomas Brutnell for the opportunity to carry out research in his lab and for guiding me throughout my time at Cornell. Also, I would like to thank my committee members, Dr. Thomas Owens and Dr. Maureen Hanson, who have provided invaluable support and advice. I am grateful for the help of the Brutnell lab members, particularly Dr. Judy Kolkman, Dr. Ruairidh Sawers, Dr. Tesfamichael Kebrom, Ms. Phyllis Farmer, Ms. Ling Xu and Mr. Kevin Ahern who all took an active role in my thesis project. As well, I would like to acknowledge the work of my collaborators, Dr. Wojciech Majeran and Dr. Klaas van Wijk without whom the proteomic analysis would not have been possible. I would also like to thank Dr. Ling Bai, Dr. Liza Conrad, and Dr. Moira Sheehan for their invaluable advice and discussions as fellow graduate students.

This work was supported by funding from the National Science Foundation (DBI-0211935) to T.P.B. and the Natural Sciences and Engineering Research Council (Canada) in the form of scholarship funds to S.C.

TABLE OF CONTENTS

LIST OF FIGURES

LIST OF TABLES

LIST OF ABBREVIATIONS

1D-SDS-PAGE; one-dimension sodium dodecyl sulfate-polyacrylamide gel electrophoresis

Ac; Activator transposon

BS; bundle sheath

bsd2; *bundle sheath defective2*

HCF136; high chlorophyll fluorescence136

M; mesophyll

PCR; polymerase chain reaction

PSII; photosystem II

WT; wild-type

Zm; *Zea mays*

CHAPTER ONE

C_4 PHOTOSYNTHESIS: MECHANISM AND REGULATION

BACKGROUND

C_4 photosynthesis is a carbon concentrating mechanism used by many dicot and monocot species to counteract energy loss to photorespiration (Edwards and Walker, 1983). By elevating carbon dioxide (CO_2) levels near ribulose-1,5-bisphosphate carboxylase oxygenase (Rubisco), C_4 species increase their photosynthetic, water and nitrogen use efficiencies in warm environments relative to their C_3 counterparts (Edwards et al., 2001). Many tropical grasses important for world agriculture perform C_4 photosynthesis, including maize, sugarcane, and sorghum, and overall, 30% of global grain production is accounted for by C_4 crop species (Steffen et al., 2005). This large impact on human nutrition has spurred renewed interest in C_4 development because of concern for potential negative effects from global climate change on world food production. Additionally, the predicted energy crisis has generated interest in C_4 regulation because many promising biofuel feedstocks, such as *Miscanthus* x *giganteus* and *Panicum virgatum* (switchgrass), operate C_4 photosynthesis. Thus, understanding mechanisms by which the C_4 syndrome is established and maintained is an important step toward engineering higher yielding plants for both food and fuel.

C_4 PHOTOSYNTHESIS UTILIZES DISTINCT PHOTOSYNTHETIC CELLS

C_4 photosynthesis is realized through biochemical and anatomical adjustments that effectively concentrate CO_2 in the vicinity of Rubisco (Edwards and Walker, 1983). Canonical C_4 species have two photosynthetic

cell types, mesophyll (M) and bundle sheath (BS), that form concentric rings around the vasculature in an arrangement known as Kranz anatomy (Nelson and Langdale, 1989). Within these cell types, carbon is fixed twice, once as a C_4 dicarboxylic acid in M cells and a second time via Rubisco in BS cells (Edwards and Walker, 1983). In maize, the carbon cycle begins in the M cells when CO_2 is hydrated by carbonic anhydrase (CA), which converts CO_2 to bicarbonate (HCO_3^-) (Edwards and Walker, 1983). HCO_3^- is then fixed by phosphoenolpyruvate carboxylase (PEPC) to form oxaloacetate (OAA) (Figure 1.1) (Hatch and Slack, 1966; Slack and Hatch, 1967; Edwards and Walker, 1983). OAA is transported from the cytosol to the plastid (Leegood, 2002), where it is converted to malate by NADP-malate dehydrogenase (NADP-MDH) (Hatch and Slack, 1969; Johnson and Hatch, 1970). Malate is then transported across the M chloroplast inner membrane (Taniguchi et al., 2004) and diffuses via plasmodesmata to the BS cells (Leegood, 2002). It is then transported into the BS plastid (Leegood, 2002), where CO_2 is released by NADP-malic enzyme (NADP-ME) (Slack and Hatch, 1967; Hatch and Kagawa, 1974). The released carbon is fixed by Rubisco to ribulose-1,5-bisphosphate as the first step in the photosynthetic carbon reduction cycle, and pyruvate yielded by decarboxylation moves to the M cells via diffusion through plasmodesmata and transport into the plastid (Leegood, 2002). The C_4 cycle is completed by the conversion of pyruvate to PEP by pyruvate, orthophosphate dikinase (PPDK) at the expense of two ATP per molecule CO_2 fixed (Hatch and Slack, 1967, 1968; Edwards and Walker, 1983).

The unique characteristics of M and BS cells also extend to plastid photochemistry and morphology. M plastids contain granal stacks, perform linear electron transport and photoreduce $NADP^+$ (Andersen et al., 1972). The

Figure 1.1. Schematic diagram showing C_4 biochemistry in the mesophyll and bundle sheath cells of maize, an NADP-ME type plant. Abbreviations: PEP (phosphoenolpyruvate), PEPC (phosphoenolpyruvate carboxylase), OAA (oxaloacetate), MDH (malate dehydrogenase), MAL (malate), ME (malic enzyme), Rubisco (ribulose-1,5-bisphosphate carboxylase oxygenase), 3-PGA (3-phosphoglycerate), Triose-P (Triose-phosphate), RuBP (Ribulose-1,5-bisphosphate), PYR (pyruvate), PPdK (pyruvate, orthophosphodikinase). Black boxes represent plasmodesmata. Ovals represent chloroplasts.

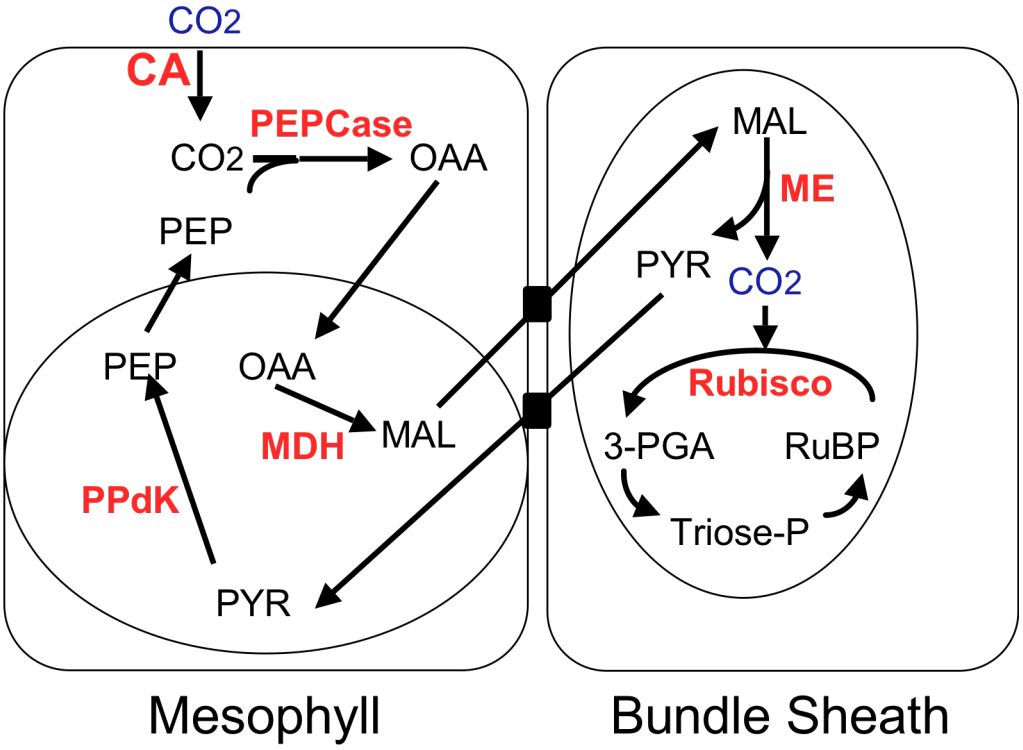
CO2
CA
PEPCase
CO2
OAA
PEP
PEP
OAA
MDH
MAL
PPdK
PYR
MAL
ME
PYR
CO2
Rubisco
3-PGA
RuBP
Triose-P
Mesophyll
Bundle Sheath

plastids themselves are randomly arranged within M cells and accumulate little or no starch (Edwards and Walker, 1983). In contrast, maize BS plastids are centrifugally arranged in proximity to the M cell wall (Edwards and Walker, 1983), lack granal stacks (Andersen et al., 1972; Kirchanski, 1975; Miller et al., 1977), are photosystem II (PSII)-depleted (Schuster et al., 1985) and perform most Calvin cycle reactions (Chollet, 1973; Kagawa and Hatch, 1974). Additionally, BS chloroplasts are believed to be restricted to cyclic electron transport due to the absence of functional PSII (Gregory et al., 1979; Ghirardi and Melis, 1983; Romanowska et al., 2006). Thus, as a result of this specialization, proper functioning of maize M and BS cells is dependent on metabolic cooperation. Specifically, M cell-generated reducing power in the form of NADPH is necessary for Calvin cycle operation in BS cells (Edwards and Walker, 1983), and the regeneration of $NADP^+$ is essential for proper photosynthetic electron transport (PET) function in M cells.

Partitioning of photosynthetic activities between M and BS cell types is mediated by cell-specific localization of many transcripts and proteins (Langdale and Nelson, 1991; Sheen, 1999). In maize, transcripts encoding PEPC, PPDK, and MDH are restricted to M cells and those encoding NADP-ME, LSU, and SSU are limited to the BS (Sheen, 1999). A number of photosynthesis-related transcripts are also known to differentially accumulate between M and BS cells such as those encoding PSII complex proteins in M cells and stress inducible genes in the BS (Furumoto et al., 2000). Recently, the suite of differentially accumulated maize genes and proteins was significantly expanded by cell-specific transcript and proteomic profiling (Majeran et al., 2005; Sawers et al., 2007). Microarray analysis indicated 1278 transcripts with either M- or BS-enriched expression patterns and predicted that 18% of the

transcriptome differentially accumulates (Sawers et al., 2007). The proteomics data established 125 BS:M stromal chloroplast expression ratios and postulated that many differences in metabolic differentiation are explained by these cells' inherent imbalance in reducing equivalent availability (Majeran et al., 2005). For example, phosphoglycerate kinase, an enzyme involved in the reducing phase of the Calvin cycle, is preferentially located in M cells where NADPH is readily available rather than in the BS. Thus, we can infer that cell-specific localization of many transcripts and proteins has been optimized for photosynthetic efficiency over time.

C_4 PHOTOSYNTHESIS EVOLVED FROM A BASAL C_3 STATE

Current models propose that C_4 biology evolved from a basal C_3 state via the recruitment and novel expression of genes already present in the genome (Sage, 2004). The transition between C_3 and C_4 photosynthesis is predicted to have occurred at least 45 times in 19 families of monocot or dicot lineages (Sage, 2004). At least three major classes of C_4 plants have been described (NAD-ME, NADP-ME, PEPCK), as well as C_3-C_4 intermediates such as in the *Cleome*, *Flaveria*, and *Heliotropium* genera (Ku et al., 1983; Marshall et al., 2007; Vogan et al., 2007) and even single cell C_4 species in the Chenopodiaceae family (Voznesenskaya et al., 2001) and a marine diatom (Reinfelder et al., 2000; Reinfelder et al., 2004).

A central question in C_4 biology is how did the multitude of C_4 subtypes evolve? Recent studies in tobacco, a C_3 plant, have shown that the decarboxylating enzymes NAD-ME, NADP-ME, and phosphoenolpyruvate carboxykinase (PEPCK) are highly active in stem and petiole BS cells and are capable of decarboxylating malate and fixing carbon to form sugars in these C_3

cells (Hibberd and Quick, 2002). These data suggest that the development of C_4 biochemistry and anatomy is evolutionarily plastic and involves modification of existing pathways rather than *de novo* creation.

In support of this view, genes encoding PPDK, PEPC, and NADP-ME are present in both C_3 and C_4 *Flaveria* species, but their expression varies between them. For example, *Ppdk* is a single copy gene present in a spectrum of C_3, C_3-C_4 intermediate, and C_4 *Flaveria* species, and its abundance is correlated with the degree of C_4 characteristics displayed in each species (Rosche et al., 1994). PEPC is a member of a gene family with both C_3 and C_4 isoforms, and the latter contains a *cis*-regulatory element in its promoter that confers C_4-type spatial regulation (Stockhaus et al., 1994; Stockhaus et al., 1997; Gowik et al., 2004; Akyildiz et al., 2007). As a result, the C_4 isoform is abundantly expressed in M cells of *Flaveria trinervia*, a C_4 species, but its orthologue in the C_3 species *Flaveria pringlei* is weakly expressed in a non cell-specific manner. *Flaveria* NADP-ME is encoded by a small gene family that includes the paralogous *Me1* and *Me2* genes (Marshall et al., 1996). *Me2* is weakly expressed in both photosynthetic and non-photosynthetic tissues. In contrast, *Me1* expression positively correlates with the degree of C_4 photosynthesis, suggesting the gene has undergone subfunctionalization. C_4 photosynthetic expression of *Me1* is *cis*-regulated by elements both upstream and downstream of the coding region, which act in BS cells to enhance expression (Marshall et al., 1997).

Extensive studies have also been performed in maize to better understand C_4 transcript regulation. Factors leading to the spatial regulation of a limited number of transcripts encoding PEPC (Langdale et al., 1991; Schaffner and Sheen, 1992), PPDK (Sheen, 1991), and *Rbcs* (Schaffner and

Sheen, 1991) have been identified. Cell-specific accumulation of PEPC transcript correlates with demethylation of a site over 3 kb upstream of its coding region (Langdale et al., 1991). Expression of C_3 and C_4 PPDK genes is derived from overlapping transcripts at the same locus and is controlled by a dual promoter system (Sheen, 1991). The C_4 PPDK promoter is sufficient to confer M cell-specificity (Taniguchi et al., 2000) and a *cis*-element has been defined (Matsuoka and Numazawa, 1991). *Rbcs* cell-specificity is controlled by many factors, including a light dependent enhancer element responsible for BS cell enrichment as well as 5′ and 3′ silencers that interact with the *trans*-acting repressor TRM1 to suppress M cell expression (Schaffner and Sheen, 1991; Viret et al., 1994; Purcell et al., 1995; Xu et al., 2001). However, the general mechanism(s) by which C_4 photosynthetic expression patterns are established on a genome-wide scale remains elusive.

UNKNOWN SIGNAL(S) INITIATE C_4 EXPRESSION PATTERNS

Light is a major factor in the establishment of the C_4 syndrome, but how the signal(s) is mediated is unknown. In the single cell C_4 species *Borszczowia aralocaspica* (Chenopodiaceae), light induces development of dimorphic chloroplasts and C_4 expression patterns (Voznesenskaya et al., 2004). In maize, light is required for establishment of C_4 patterns of PPDK, PEPC, NADP-MDH, NADP-ME and Rubisco expression (Sheen and Bogorad, 1987; Purcell et al., 1995). Both M and BS cells express Rubisco in the dark, but an *Rbcs* enhancer element is induced by red/far-red light in BS cells and a repressor element is activated by blue light in M cells (Purcell et al., 1995), resulting in the spatial restriction of Rubisco to BS cells in the light. However, light is not solely responsible for development of the C_4 syndrome, since *Rbcs* will

eventually localize to BS tissues after extended growth in darkness (J. Langdale, unpublished).

Maize M and BS cells arise from different cell lineages, and positional cues play an important role in their differentiation (Dengler et al., 1985). This signal appears to be local since BS cells develop in the same order that veins are formed (Dengler et al., 1985), yet their differentiation is asynchronous around the vein (Langdale et al., 1988a). Additionally, evidence from a recent comparative analysis of C_3, C_3-C_4 intermediate, and C_4 *Flaveria* species indicates that Kranz anatomy and vein patterning precede M and BS C_4 expression patterns (McKown and Dengler, 2007). In maize, the positional cue is relatively more important than light in M cells that are distant from a vein, since they do not accumulate C_4 enzymes (Langdale et al., 1988b). This hypothesis is supported by the observation that distance from the vein positively influences Rubisco accumulation in M cells, specifically when more than two or three M cells lie between adjacent veins. Distant M cells also fail to accumulate PEPC, PPDK, and NADP-ME, suggesting they follow a basal C_3 developmental pattern. Additionally, previous research in maize shows that C_4 mRNA accumulation peaks with the development of Kranz anatomy, supporting the notion of a positional signal in this species (Langdale et al., 1988a). This signal may be a metabolite emanating from the vasculature that elicits cell fate along a concentration gradient as it diffuses across cell layers (Langdale et al., 1988b).

A recent model on the establishment of C_4 photosynthesis takes this idea a step further and proposes that after signals for M and BS differentiation are perceived, extant C_3 regulatory pathways are harnessed to establish and maintain these cell types (Sawers et al., 2007). As discussed above, current

models of C_4 development propose the existence of cell-specific *cis* and *trans* regulatory factors, some which have already been identified. However, RNA profiling data indicate that nearly 18% of the maize leaf transcriptome is differentially expressed between M and BS cells, and it is unlikely that common regulatory elements were recruited for this vast number of genes (Sawers et al., 2007). Instead, key changes may result in novel cellular environments in the M and BS cells such as differential complex formation, redox potential and sugar and energy metabolite concentrations that then feedback to the nucleus and control networks of genes through existing C_3 regulatory pathways. For example, differential accumulation of PSII in M cells may control nuclear gene expression via the production of reactive oxygen species, a class of known signaling molecules (Beck, 2005). These signals would be absent in the BS because functional PSII never develops and therefore would have no impact in establishing nuclear gene expression in that cell type. This scenario greatly simplifies the number of modifications necessary to induce evolution of the C_4 syndrome, consistent with its plastic and frequent occurrence in Nature. Maize mutants defective in establishing C_4 photosynthesis can be used to test and refine this hypothesis.

MUTANTS MAY BE USED TO DISSECT C_4 CELL DEVELOPMENT

A number of maize photosynthetic mutants have been successfully used to gain insight into mechanisms of M and BS cell differentiation. One such mutant, *argenti*a (*ar*), greens along the veins first so that both green and predominantly white mutant leaf tissue are available for analysis of C_4 enzyme accumulation (Langdale et al., 1987). With the exception of MDH, C_4 enzyme levels are lower in predominantly white *ar* leaf blades compared to

green *ar* leaves and their accumulation levels remain constant throughout the leaf. This is in contrast to WT plants, which have increasing C_4 protein abundance in a gradient from base to tip. In addition, predominantly white *ar* leaves have delayed BS cell development and accumulate C_4 proteins later than M cells. This developmental delay is at the level of transcription since mRNA and protein accumulation patterns coincide (Langdale et al., 1988a). Again, this pattern is in contrast with that of green sectors in *ar* leaves and WT tissues, which both accumulate cell-specific mRNAs in BS cells before M cells. The authors used this mutational analysis to determine a number of key points in M and BS cell development: (1) compartmentalization of C_4 enzymes is controlled by RNA accumulation levels, (2) M and BS cells can behave autonomously, (3) differentiation occurs preferentially in areas of established Kranz anatomy, and (4) that M and BS cells interact early in development. Their conclusions led to the hypothesis of a dual repressor/stimulator model, which was subsequently found to control *Rbcs* expression as described above.

Mutational analysis of the nuclear maize mutant *plastids undifferentiated* (*pun*) revealed that functional chloroplasts are not required for light-enhanced positional cues involved in M and BS differentiation nor are they required to establish appropriate spatial regulation of Rubisco (Roth et al., 2001). In *pun* mutants, BS and M chloroplast biogenesis is disrupted very early in development, and chloroplasts never form internal membranes or accumulate thylakoid-associated photosynthetic proteins in the light or dark. Despite this, RNA levels of the C_4 carbon shuttle enzymes are similar to WT, and *in situ* hybridization shows that *rbcL* and *Rbcs* spatial regulation is maintained but with reduced transcript levels. This is particularly interesting since plastid function depends on the coordination of gene expression between two

different genomes, the nucleus and the plastid (Taylor, 1989). The nucleus is predicted to encode almost 3500 plastid targeted proteins (van Wijk, 2004). In contrast, the maize plastome (NC_001666) encodes only 111 proteins, including *rbcL*. Consequently, chloroplasts must carefully orchestrate photosynthetic complex formation and the activity of both nuclear- and plastid-encoded gene products (Fey *et al.*, 2005). As a result, it is significant that the accumulation of classically defined C_4 enzymes is not dependent on the functional state of the plastid, because this indicates that regulatory control must be derived from some external signal during development, such as the positional signal coming from the vein. In addition, results from the analysis of *pun* suggest that mutants disrupted in photosynthesis or plastid development will not be sufficient to dissect M and BS cell differentiation on a genomic scale. Rather, mutants such as *ar* that decouple M and BS cell differentiation are necessary to gain further insight into this developmental program. Alternatively, a comparative analysis of maize mutants disrupted in cell-specific activities, such as PSII or Rubisco assembly, can identify suites of genes responding to extant C_3 signaling pathways in M and BS cells.

BS CELL MUTANTS HAVE BEEN IDENTIFIED

The first genetic screen to identify cell-specific photosynthetic defects in maize resulted in the identification of a series of *bundle sheath defective* mutants in which M cells appear to differentiate normally (Hall et al., 1998a). Microscopic and immunoblot analysis revealed ten lines with specific defects in BS cell morphology and C_4 enzyme accumulation during a systematic screen of 122 pale green mutants. These mutants were divided into 3 non-allelic classes, *bsd1, bsd2,* and *bsd3*, the latter of which has not been fully

characterized. Phenotypic data show that *bsd1* BS plastids have rudimentary lamellae and fail to accumulate ME and Rubisco transcripts and proteins in the leaf base (Langdale and Kidner, 1994; Rossini et al., 2001). However, *bsd1* is not a true BS mutant, even though its primary phenotypic defect is an altered BS plastid structure. Rather, *Bsd1* encodes a transcriptional regulator of plastid biogenesis, whose action is light and cell-independent (Hall et al., 1998b; Cribb et al., 2001). Dark-grown *bsd1* fails to accumulate Rubisco in both M and BS cell types, although in WT both cell types accumulate Rubisco in darkness. In addition, *Bsd1* transcript accumulates in both C_3 and C_4 type tissues in the light, and *bsd1* mutants recover in the leaf tip. Therefore, *bsd1* is not selectively disrupted in BS cell formation.

The *bsd2* mutant provides a more complete disruption of BS cell differentiation. BSD2 protein is proposed to act as a post-translational regulator of Rubisco large subunit accumulation and its sequence is highly similar to structural motifs seen in Dna-J chaperone family members (Roth et al., 1996; Hall et al., 1998a; Brutnell et al., 1999). In *bsd2*, loss of this chaperone activity leads to ectopic accumulation of polysome-associated *rbcL* in M cells and dark-grown etiolated tissue. Thus, BSD2 likely functions in the removal of nascent *rbcL* polypeptides from plastid polysomes. In addition, the loss of BSD2 function results in a failure to accumulate large and small Rubisco subunits, presumably because *rbcL* polypeptides are unavailable for holoenzyme formation. Consequently, *bsd2* mutants cannot perform Calvin cycle activities (Smith et al., 1998) and die when seedling reserves are exhausted. Expression data suggest *Bsd2* is required in both M and BS cell types, but whether its chaperone activity enables the accumulation of *rbcL* in BS cells and/or its destruction in M cells is unclear. Unfortunately, the specific

mode and site of action for this chaperone is unresolved, largely due to difficulties in antibody production (T. Brutnell, personal communication). Nevertheless, *bsd2* is the most selectively disrupted BS cell mutant available in maize.

M CELL MUTANTS HAVE BEEN IDENTIFIED

A number of M cell-specific maize mutants are available from EMS screens but were not specifically identified as such at the time of their discovery. *hcf2, hcf3* (Miles and Daniel, 1974), *hcf19G* and *hcf19YG* (Leto and Miles, 1980) all have presumptive M cell-specific defects because they are blocked in PSII electron transport as determined by fluorescence kinetics. As described above, functional PSII is limited to the M cell, and therefore a disruption in its formation or operation leads to a *de facto* M cell-specific defect. Protein studies of *hcf3, hcf19G* and *hcf19YG* revealed they lack two core subunits of PSII, D1 and Cytochrome b559 (Leto and Miles, 1980). In addition, electron microscopy studies of *hcf2* and *hcf3* show defective M cell grana formation (Miles and Daniel, 1974). However, the specific genetic lesions of these M cell mutants are unknown, and therefore their utility in understanding C_4 development is limited.

Recently, a M cell-specific gene was tagged and cloned in a large-scale mutagenesis project utilizing the *Ac*/Ds transposable element system (Kolkman et al., 2005). The insertion of *Ac* yielded a recessive seedling lethal mutation in *high chlorophyll fluorescence136* (*hcf136)*, a PSII stability or assembly factor previously characterized in *Arabidopsis* (Meurer et al., 1998; Plucken et al., 2002). As discussed in Chapter Two, Zm *hcf136* is a M cell-specific mutant that lacks PSII protein function and accumulation as well as thylakoid grana

formation in M plastids. *hcf136* M chloroplasts also have a specific defect in processing the *psbB-psbT-psbH-petB-petD* polycistron. Additionally, *Hcf136* gene expression is restricted to M cells, and thus the mutant's phenotype stems from a true disruption of M cell activity. Thus, *hcf136* and *bsd2* are ideally suited for in depth comparative studies of C_4 gene expression.

GLOBAL TRANSCRIPT ANALYSIS OF M AND BS MUTANTS

The availability of BS and M specific mutants provides an opportunity to test the hypothesis that cellular environment plays an important role in differentiation of C_4 photosynthetic cells. As described above, a recent transcript profiling experiment suggests that 18% of the maize leaf transcriptome is differentially expressed between M and BS cells (Sawers et al., 2007). The authors suggest these transcriptional profiles result from a few key regulatory changes coupled with the differential accumulation of cellular factors such as photosynthetic protein complexes, sugar and energy metabolites, and plastid redox poise. Thus, as a result of cellular environment, different extant C_3 signaling networks would be initiated in BS and M cells and would lead to feedback loops that establish observed BS:M expression patterns. The relative importance of any or all of these cellular factors in differentiation can be addressed by global transcriptional profiling of the cell-specific mutants *hcf136* and *bsd2*.

Leaf tissue of *hcf136* mutants does not accumulate PSII or operate linear electron transport, nor does it produce sugars in BS cells. *bsd2* lacks Rubisco (Roth et al., 1996; Brutnell et al., 1999) and Calvin cycle activity (Smith et al., 1998), and has a more reduced PQ pool in its M cells (Chapter Three). Thus, when comparing phenotypes between these two mutants, lack of sugar

production in BS cells is a shared quality, and PET protein accumulation (e.g. OEC and PSII in M cell plastids) and plastid redox state (e.g. PQ pool, NADPH:$NADP^+$) are distinguishing characteristics in the M. Thus, genes with similar transcriptional profiles in both *hcf136* and *bsd2* are likely responding to the sugar state of the BS cell, and those with inverse profiles are likely responding to PET protein accumulation or plastid redox state in M cells. Thus, the availability of well-defined M and BS mutants provides an opportunity to test the hypothesis that cellular environmental factors are important in establishing differential BS:M expression profiles.

To assess the importance of cell environmental factors, global transcriptional profiling was performed using microarray technology. The platform currently available is a 70-mer oligonucleotide array produced by the Maize Array Project Consortium at the University of Arizona (maizearray.org). This array consists of approximately 60,000 oligonucleotide features designed with redundancy to expressed sequence tags (EST) assembled by The Institute for Genomic Research. Consequently, many genes are represented by multiple features, and gene family members may not be distinguishable. However, this platform can be used to identify thousands of differentially expressed features, and these profiles can be used to distinguish trends in the data.

M and BS cells of WT and mutant siblings were isolated by enzymatic and mechanical digestion, respectively, and hybridized to the Maize Arizona Oligonucleotide Array. To avoid confounding treatment effects associated with differences in the cell isolation methods, dual label hybridizations were performed only within cell type between WT and mutant tissues. In total, four different experiments were performed: (1) *hcf136* M vs. WT M, (2) *hcf136* BS vs.

WT BS, (3) *bsd2* M vs. WT M, and (4) *bsd2* BS vs. WT BS. For each experiment, six biological replicates were performed, and a moderated t-test was used to identify differentially expressed features from the normalized data. This experimental design addresses the impact of cellular environment by allowing direct comparison of all M cell or BS cell data and indirect comparisons between cell types.

Before comparative surveys of *hcf136* and *bsd2* transcript profiles were performed, each experiment was treated to independent analysis to identify mutant-specific trends in gene expression. These independent analyses of *hcf136* and *bsd2* are discussed in detail in Chapters Two and Three, respectively. In summary, M and BS cells appear to operate predominately autonomous transcriptional networks. In *hcf136*, 2580 and 1669 features are differentially expressed at a 5% false discovery rate (FDR) in M and BS cell experiments respectively, but only 577 identified features are differentially expressed in both cell types (Chapter Two). In *bsd2*, the lack of common features is more dramatic. Only 34 differentially expressed features are common to M and BS cells, which individually have 60 and 568 differentially expressed features, respectively, at 5% FDR. Additionally, each mutant displays a larger transcriptional response in the cell of primary defect, and the directionality of this response is nonrandom. Transcripts in *hcf136* M cells tend to be up-regulated while transcripts in *bsd2* BS cells are down-regulated. Thus, M and BS cells respond almost uniquely to the selective loss of Rubisco or PSII.

In light of the nearly autonomous regulation of M and BS transcription, it is important to consider these cell types separately in determining potential signals. Therefore, M- and BS-enriched features were independently analyzed

for alterations in BS:M differential expression ratios in a preliminary comparison between WT, *bsd2*, and *hcf136*. Results of this comparative survey show that BS:M of M-enriched features tend to respond differently in *hcf136* and *bsd2*, but BS:M of BS-enriched features tend to decrease or increase in the same direction in both mutants. Thus, it appears that M-enriched features are responding to a distinguishing characteristic between these mutants, such as photosynthetic protein accumulation or plastid redox state. In contrast, BS-enriched features are generally responding to a shared quality, and therefore their expression is likely controlled by sugar metabolite concentrations. Thus, comparative global transcriptional profiling has provided evidence for the use of cellular environmental factors in the control of C_4 differentiation in maize.

IMPLICATIONS FOR FUTURE WORK IN C_4 BIOLOGY

The idea of cellular environmental factors leading to C_4 differentiation has broad implications for future work in C_4 biology, because it implies that large C_4-like transcriptional changes can be elicited with few alterations to C_3 plants. Thus, data presented in this thesis provide an optimistic result for the development of C_4 rice, which is highly desirable because yields can no longer meet demand without a significant increase in photosynthetic capacity (Mitchell and Sheehy, 2006). Previous efforts to import C_4 photosynthesis into rice, a C_3 plant, have focused on over-expressing classically defined C_4 enzymes such as PEPC (Ku et al., 1999). However, these efforts have been largely unsuccessful in changing BS:M expression patterns. Indeed, changes to C_4 enzyme differential expression patterns are notably muted in *hcf136* and *bsd2*, with the exception of Rubisco in both mutants and ME in *bsd2*. Therefore, CA, PEPC, MDH and PPDK may represent key regulatory changes that enable

C_4 photosynthesis but do not act in the extant C_3 signaling networks because they possess *de novo* functions in a C_4 context. In contrast, BS:M expression of *Rbcs* and *Me* may be reduced in the mutants because their function, and presumably their associated regulatory networks, have remained intact during the transition from C_3 to C_4. Thus, efforts to develop C_4 rice should focus on understanding the signaling networks controlling the suites of genes with altered BS:M in *hcf136* and *bsd2*. Identifying how these groups respond to their signals may simplify the number of genetically engineered traits necessary to achieve C_4 rice and would be an important step forward in our abilities to breed higher yielding plants to attain food security.

LITERATURE CITED

Akyildiz, M., Gowik, U., Engelmann, S., Koczor, M., Streubel, M., and Westhoff, P. (2007). Evolution and function of a *cis*-regulatory module for mesophyll-specific gene expression in the C_4 dicot *Flaveria trinervia*. Plant Cell **in press**.

Andersen, K.S., Bain, J.M., Bishop, D.G., and Smillie, R.M. (1972). Photosystem II activity in agranal bundle sheath chloroplasts from *Zea mays*. Plant Physiol **49,** 461-466.

Beck, C.F. (2005). Signaling pathways from the chloroplast to the nucleus. Planta **222,** 743-756.

Brutnell, T.P., Sawers, R.J., Mant, A., and Langdale, J.A. (1999). BUNDLE SHEATH DEFECTIVE2, a novel protein required for post-translational regulation of the *rbcL* gene of maize. Plant Cell **11,** 849-864.

Chollet, R. (1973). Photosynthetic carbon metabolism in isolated maize bundle sheath strands. Plant Physiol **51,** 787-792.

Cribb, L., Hall, L.N., and Langdale, J.A. (2001). Four mutant alleles elucidate the role of the G2 protein in the development of C_4 and C_3 photosynthesizing maize tissues. Genetics **159,** 787-797.

Dengler, N.G., Dengler, R.E., and Hattersley, P.W. (1985). Differing ontogenetic origins of PCR (Kranz) sheaths in leaf blades of C_4 grasses (Poaceae). Amer J Bot **72,** 284-302.

Edwards, G.E., and Walker, D. (1983). C_3, C_4: Mechanisms, cellular and environmental regulation of photosynthesis. (Berkeley: University of California Press).

Edwards, G.E., Furbank, R.T., Hatch, M.D., and Osmond, C.B. (2001). What does it take to be C_4? Lessons from the evolution of C_4 photosynthesis. Plant Physiol **125,** 46-49.

Fey, V., Wagner, R., Brautigam, K., and Pfannschmidt, T. (2005). Photosynthetic redox control of nuclear gene expression. J Exp Bot **56,** 1491-1498.

Furumoto, T., Hata, S., and Izui, K. (2000). Isolation and characterization of cDNAs for differentially accumulated transcripts between mesophyll cells and bundle sheath strands of maize leaves. Plant Cell Physiol **41,** 1200-1209.

Ghirardi, M.L., and Melis, A. (1983). Localization of photosynthetic electron transport components in mesophyll and bundle sheath chloroplasts of *Zea mays*. Arch Biochem Biophys **224,** 19-28.

Gowik, U., Burscheidt, J., Akyildiz, M., Schlue, U., Koczor, M., Streubel, M., and Westhoff, P. (2004). *cis*-Regulatory elements for mesophyll-specific gene expression in the C_4 plant *Flaveria trinervia,* the promoter of the C_4 *phosphoenolpyruvate carboxylase* gene. Plant Cell **16,** 1077-1090.

Gregory, R.P., Droppa, M., Horvath, G., and Evans, E.H. (1979). A comparison based on delayed light emission and fluorescence induction of intact chloroplasts isolated from mesophyll protoplasts and bundle-sheath cells of maize. Biochem J **180,** 253-256.

Hall, L.N., Roth, R., Brutnell, T.P., and Langdale, J.A. (1998a). Cellular differentiation in the maize leaf is disrupted by bundle sheath defective mutations. Symp Soc Exp Biol **51,** 27-31.

Hall, L.N., Rossini, L., Cribb, L., and Langdale, J.A. (1998b). GOLDEN 2: a novel transcriptional regulator of cellular differentiation in the maize leaf. Plant Cell **10,** 925-936.

Hatch, M.D., and Slack, C.R. (1966). Photosynthesis by sugar-cane leaves. A new carboxylation reaction and the pathway of sugar formation. Biochem J **101,** 103-111.

Hatch, M.D., and Slack, C.R. (1967). The participation of phosphoenolpyruvate synthetase in photosynthetic CO_2 fixation of tropical grasses. Arch Biochem Biophys **120,** 224-225.

Hatch, M.D., and Slack, C.R. (1968). A new enzyme for the interconversion of pyruvate and phosphopyruvate and its role in the C_4 dicarboxylic acid pathway of photosynthesis. Biochem J **106,** 141-146.

Hatch, M.D., and Slack, C.R. (1969). Studies on the mechanism of activation and inactivation of pyruvate, phosphate dikinase. A possible regulatory role for the enzyme in the C_4 dicarboxylic acid pathway of photosynthesis. Biochem J **112,** 549-558.

Hatch, M.D., and Kagawa, T. (1974). NAD malic enzyme in leaves with C-pathway photosynthesis and its role in C_4 acid decarboxylation. Arch Biochem Biophys **160,** 346-349.

Hibberd, J.M., and Quick, W.P. (2002). Characteristics of C_4 photosynthesis in stems and petioles of C3 flowering plants. Nature **415,** 451-454.

Johnson, H.S., and Hatch, M.D. (1970). Properties and regulation of leaf nicotinamide-adenine dinucleotide phosphate-malate dehydrogenase and 'malic' enzyme in plants with the C_4-dicarboxylic acid pathway of photosynthesis. Biochem J **119,** 273-280.

Kagawa, T., and Hatch, M.D. (1974). C_4-acids as the source of carbon dioxide for Calvin cycle photosynthesis by bundle sheath cells of the C_4-pathway species *Atriplex spongiosa*. Biochem Biophys Res Commun **59,** 1326-1332.

Kirchanski, S.J. (1975). The ultrastructural development of the dimorphic plastids of *Zea mays* L. Amer J Bot **62,** 695–705.

Kolkman, J.M., Conrad, L.J., Farmer, P.R., Hardeman, K., Ahern, K.R., Lewis, P.E., Sawers, R.J., Lebejko, S., Chomet, P., and Brutnell, T.P. (2005). Distribution of *Activator* (*Ac*) throughout the maize genome for use in regional mutagenesis. Genetics **169,** 981-995.

Ku, M.S., Monson, R.K., Littlejohn, R.O., Nakamoto, H., Fisher, D.B., and Edwards, G.E. (1983). Photosynthetic characteristics of C_3-C_4 intermediate *Flaveria* species : I. Leaf anatomy, photosynthetic responses to O_2 and CO_2, and activities of key enzymes in the C_3 and C_4 pathways. Plant Physiol **71,** 944-948.

Ku, M.S., Agarie, S., Nomura, M., Fukayama, H., Tsuchida, H., Ono, K., Hirose, S., Toki, S., Miyao, M., and Matsuoka, M. (1999). High-level expression of maize *phosphoenolpyruvate carboxylase* in transgenic rice plants. Nat Biotechnol **17,** 76-80.

Langdale, J.A., and Nelson, T. (1991). Spatial regulation of photosynthetic development in C_4 plants. Trends Genet **7,** 191-196.

Langdale, J.A., and Kidner, C.A. (1994). *bundle sheath defective,* a mutation that disrupts cellular differentiation in maize leaves. Development **120,** 673-681.

Langdale, J.A., Metzler, M.C., and Nelson, T. (1987). The *argentia* mutation delays normal development of photosynthetic cell-types in *Zea mays*. Dev Biol **122,** 243-255.

Langdale, J.A., Rothermel, B.A., and Nelson, T. (1988a). Cellular pattern of photosynthetic gene expression in developing maize leaves. Genes Dev **2,** 106-115.

Langdale, J.A., Taylor, W.C., and Nelson, T. (1991). Cell-specific accumulation of maize *phosphoenolpyruvate carboxylase* is correlated with demethylation at a specific site greater than 3 kb upstream of the gene. Mol Gen Genet **225,** 49-55.

Langdale, J.A., Zelitch, I., Miller, E., and Nelson, T. (1988b). Cell position and light influence C_4 versus C_3 patterns of photosynthetic gene expression in maize. EMBO J **7,** 3643-3651.

Leegood, R.C. (2002). C_4 photosynthesis: principles of CO_2 concentration and prospects for its introduction into C_3 plants. J Exp Bot **53,** 581-590.

Leto, K.J., and Miles, D. (1980). Characterization of three photosystem II mutants in *Zea mays* L. lacking a 32,000 Dalton lamellar polypeptide. Plant Physiol **66,** 18-24.

Majeran, W., Cai, Y., Sun, Q., and van Wijk, K.J. (2005). Functional differentiation of bundle sheath and mesophyll maize chloroplasts determined by comparative proteomics. Plant Cell **17,** 3111-3140.

Marshall, D.M., Muhaidat, R., Brown, N.J., Liu, Z., Stanley, S., Griffiths, H., Sage, R.F., and Hibberd, J.M. (2007). *Cleome,* a genus closely related to *Arabidopsis,* contains species spanning a developmental progression from C_3 to C_4 photosynthesis. Plant J **51,** 886-896.

Marshall, J.S., Stubbs, J.D., and Taylor, W.C. (1996). Two genes encode highly similar chloroplastic NADP-malic enzymes in *Flaveria*. Implications for the evolution of C_4 photosynthesis. Plant Physiol **111,** 1251-1261.

Marshall, J.S., Stubbs, J.D., Chitty, J.A., Surin, B., and Taylor, W.C. (1997). Expression of the C_4 *Me1* gene from *Flaveria bidentis* requires an interaction between 5' and 3' sequences. Plant Cell **9,** 1515-1525.

Matsuoka, M., and Numazawa, T. (1991). *Cis*-acting elements in the *pyruvate, orthophosphate dikinase* gene from maize. Mol Gen Genet **228,** 143-152.

McKown, A.D., and Dengler, N.G. (2007). Key innovations in the evolution of Kranz anatomy and C_4 vein pattern in *Flaveria* (Asteraceae). Amer J Bot **94,** 382-399.

Meurer, J., Plucken, H., Kowallik, K.V., and Westhoff, P. (1998). A nuclear-encoded protein of prokaryotic origin is essential for the stability of photosystem II in *Arabidopsis thaliana*. EMBO J **17,** 5286-5297.

Miles, C.D., and Daniel, D.J. (1974). Chloroplast reactions of photosynthetic mutants in *Zea mays*. Plant Physiol **53,** 589-595.

Miller, K.R., Miller, G.J., and McIntyre, K.R. (1977). Organization of the photosynthetic membrane in maize mesophyll and bundle sheath chloroplasts. Biochim Biophys Acta **459,** 145-156.

Mitchell, P.L., and Sheehy, J.E. (2006). Supercharging rice photosynthesis to increase yield. New Phytol **171,** 688-693.

Nelson, T., and Langdale, J.A. (1989). Patterns of leaf development in C_4 plants. Plant Cell **1,** 3-13.

Plucken, H., Muller, B., Grohmann, D., Westhoff, P., and Eichacker, L.A. (2002). The HCF136 protein is essential for assembly of the photosystem II reaction center in *Arabidopsis thaliana*. FEBS Lett **532,** 85-90.

Purcell, M., Mabrouk, Y.M., and Bogorad, L. (1995). Red/far-red and blue light-responsive regions of maize *rbcS-m3* are active in bundle sheath and mesophyll cells, respectively. Proc Natl Acad Sci U S A **92,** 11504-11508.

Reinfelder, J.R., Kraepiel, A.M., and Morel, F.M. (2000). Unicellular C_4 photosynthesis in a marine diatom. Nature **407,** 996-999.

Reinfelder, J.R., Milligan, A.J., and Morel, F.M. (2004). The role of the C_4 pathway in carbon accumulation and fixation in a marine diatom. Plant Physiol **135,** 2106-2111.

Romanowska, E., Drozak, A., Pokorska, B., Shiell, B.J., and Michalski, W.P. (2006). Organization and activity of photosystems in the mesophyll and bundle sheath chloroplasts of maize. J Plant Physiol **163,** 607-618.

Rosche, E., Streubel, M., and Westhoff, P. (1994). Primary structure of the photosynthetic *pyruvate orthophosphate dikinase* of the C_3 plant *Flaveria pringlei* and expression analysis of *pyruvate orthophosphate dikinase* sequences in C_3, C_3-C_4 and C_4 *Flaveria* species. Plant Mol Biol **26,** 763-769.

Rossini, L., Cribb, L., Martin, D.J., and Langdale, J.A. (2001). The maize *golden2* gene defines a novel class of transcriptional regulators in plants. Plant Cell **13,** 1231-1244.

Roth, R., Hall, L.N., Brutnell, T.P., and Langdale, J.A. (1996). *bundle sheath defective2,* a mutation that disrupts the coordinated development of bundle sheath and mesophyll cells in the maize leaf. Plant Cell **8,** 915-927.

Roth, R., Sawers, R.J., Munn, H.L., and Langdale, J.A. (2001). *Plastids undifferentiated,* a nuclear mutation that disrupts plastid differentiation in *Zea mays* L. Planta **213,** 647-658.

Sage, R.F. (2004). The evolution of C_4 photosynthesis. New Phytol **161,** 341-370.

Sawers, R.J., Liu, P., Anufrikova, K., Hwang, J.T., and Brutnell, T.P. (2007). A multi-treatment experimental system to examine photosynthetic differentiation in the maize leaf. BMC Genomics **8,** 12.

Schaffner, A.R., and Sheen, J. (1991). Maize *rbcS* promoter activity depends on sequence elements not found in dicot *rbcS* promoters. Plant Cell **3,** 997-1012.

Schaffner, A.R., and Sheen, J. (1992). Maize C_4 photosynthesis involves differential regulation of *phosphoenolpyruvate carboxylase* genes. Plant J **2,** 221-232.

Schuster, G., Ohad, I., Martineau, B., and Taylor, W.C. (1985). Differentiation and development of bundle sheath and mesophyll thylakoids in maize. Thylakoid polypeptide composition, phosphorylation, and organization of photosystem II. J Biol Chem **260,** 11866-11873.

Sheen, J. (1991). Molecular mechanisms underlying the differential expression of maize *pyruvate, orthophosphate dikinase* genes. Plant Cell **3,** 225-245.

Sheen, J. (1999). C_4 gene expression. Annu Rev Plant Physiol Plant Mol Biol **50,** 187-217.

Sheen, J.Y., and Bogorad, L. (1987). Differential expression of C_4 pathway genes in mesophyll and bundle sheath cells of greening maize leaves. J Biol Chem **262,** 11726-11730.

Slack, C.R., and Hatch, M.D. (1967). Comparative studies on the activity of carboxylases and other enzymes in relation to the new pathway of photosynthetic carbon dioxide fixation in tropical grasses. Biochem J **103,** 660-665.

Smith, L.H., Langdale, J.A., and Chollet, R. (1998). A functional Calvin cycle is not indispensable for the light activation of C_4 phosphoenolpyruvate carboxylase kinase and its target enzyme in the maize mutant *bundle sheath defective2-mutable1*. Plant Physiol **118,** 191-197.

Steffen, W., Sanderson, A., Tyson, P., Jager, J., Matson, P., Moore III, B., Oldfield, F., Richarson, K., Schellnhuber, H.J., Turner II, B.L., and Wasson, R.J. (2005). Global change and the Earth system: A planet under pressure. (Berlin: Springer).

Stockhaus, J., Poetsch, W., Steinmuller, K., and Westhoff, P. (1994). Evolution of the C_4 *phosphoenolpyruvate carboxylase* promoter of the C_4 dicot *Flaveria trinervia*: an expression analysis in the C_3 plant tobacco. Mol Gen Genet **245,** 286-293.

Stockhaus, J., Schlue, U., Koczor, M., Chitty, J.A., Taylor, W.C., and Westhoff, P. (1997). The promoter of the gene encoding the C_4 form of *phosphoenolpyruvate carboxylase* directs mesophyll-specific expression in transgenic C_4 *Flaveria* spp. Plant Cell **9,** 479-489.

Taniguchi, M., Izawa, K., Ku, M.S., Lin, J.H., Saito, H., Ishida, Y., Ohta, S., Komari, T., Matsuoka, M., and Sugiyama, T. (2000). The promoter for the maize C_4 *pyruvate, orthophosphate dikinase* gene directs cell- and tissue-specific transcription in transgenic maize plants. Plant Cell Physiol **41,** 42-48.

Taniguchi, Y., Nagasaki, J., Kawasaki, M., Miyake, H., Sugiyama, T., and Taniguchi, M. (2004). Differentiation of dicarboxylate transporters in mesophyll and bundle sheath chloroplasts of maize. Plant Cell Physiol **45,** 187-200.

Taylor, W.C. (1989). Regulatory interactions between nuclear and plastid genomes. Annu Rev Plant Physiol Plant Mol Biol **40,** 211-233.

van Wijk, K.J. (2004). Plastid proteomics. Plant Physiol Biochem **42,** 963-977.

Viret, J.F., Mabrouk, Y., and Bogorad, L. (1994). Transcriptional photoregulation of cell-type-preferred expression of maize *rbcS-m3*: 3' and 5' sequences are involved. Proc Natl Acad Sci U S A **91,** 8577-8581.

Vogan, P.J., Frohlich, M.W., and Sage, R.F. (2007). The functional significance of C_3-C_4 intermediate traits in *Heliotropium* L. (Boraginaceae): gas exchange perspectives. Plant Cell Environ **30,** 1337-1345.

Voznesenskaya, E.V., Franceschi, V.R., and Edwards, G.E. (2004). Light-dependent development of single cell C_4 photosynthesis in cotyledons of *Borszczowia aralocaspica* (Chenopodiaceae) during transformation from a storage to a photosynthetic organ. Ann Bot (Lond) **93,** 177-187.

Voznesenskaya, E.V., Franceschi, V.R., Kiirats, O., Freitag, H., and Edwards, G.E. (2001). Kranz anatomy is not essential for terrestrial C_4 plant photosynthesis. Nature **414,** 543-546.

Xu, T., Purcell, M., Zucchi, P., Helentjaris, T., and Bogorad, L. (2001). TRM1, a YY1-like suppressor of *rbcS-m3* expression in maize mesophyll cells. Proc Natl Acad Sci U S A **98,** 2295-2300.

CHAPTER TWO

DE-REGULATION OF MAIZE C_4 PHOTOSYNTHETIC DEVELOPMENT IN A MESOPHYLL CELL DEFECTIVE MUTANT*

ABSTRACT

During *Zea mays* (maize) C_4 differentiation, mesophyll (M) and bundle sheath (BS) cells accumulate distinct sets of photosynthetic enzymes, with very low photosystem II (PSII) content in BS chloroplasts. Consequently, there is little linear electron transport in the BS and ATP is generated by cyclic electron flow. In contrast, M thylakoids are very similar to those of C_3 plants and produce the ATP and NADPH that drive metabolic activities. Regulation of this differentiation process is poorly understood but involves expression and coordination of nuclear and plastid genomes. Here, we identify a recessive allele of the maize *Hcf136* homologue that in *Arabidopsis thaliana* functions as a PSII stability or assembly factor located in the thylakoid lumen. Proteome analysis of the thylakoids and electron microscopy reveal that Zm *hcf136* lacks PSII complexes and grana thylakoids in M chloroplasts, consistent with the previously defined *Arabidopsis* function. Interestingly, *hcf136* is also defective in processing the full-length *psbB-psbT-psbH-petB-petD* polycistron specifically in M chloroplasts. To determine whether the loss of PSII in M cells affects C_4 differentiation, we performed cell-type specific transcript analysis of *hcf136* and wild-type seedlings. The results indicate that M and BS cells respond uniquely to the loss of PSII, with little overlap in gene expression changes

* Proteomics was performed by Dr. Wojciech Majeran (van Wijk Lab; Cornell University). Microarray statistical analysis was performed by Dr. Peng Liu (Iowa State University). Fv/Fm measurements were performed by Dr. Tom Owens (Cornell University). *Hcf136* was mapped by Phyllis Farmer (Brutnell Lab). *Hcf136* was identified by Dr. Judy Kolkman (Cornell University).

between data sets. These results are discussed in the context of signals that may drive differential gene expression in C_4 photosynthesis.

INTRODUCTION

In *Zea mays* (maize), photosynthetic activities are partitioned between two morphologically and biochemically distinct cell types, mesophyll (M) and bundle sheath (BS) (Edwards and Walker, 1983). M and BS cells are organized as concentric files around the vasculature in a classical Kranz anatomy. Functionally, these two cell-types cooperate in photosynthesis, carbon fixation (Edwards et al., 2001b; Majeran et al., 2005), nitrogen metabolism (Rathnam and Edwards, 1975, 1976; Harel et al., 1977; Becker et al., 1993) and sulfur assimilation (Burgener et al., 1998). Notably, M plastids contain grana thylakoids, perform linear electron transport and photoreduce $NADP^+$ (Andersen et al., 1972). In contrast, BS chloroplasts are agranal (Andersen et al., 1972; Kirchanski, 1975; Miller et al., 1977), PSII-depleted (Schuster et al., 1985) and perform most of the reactions of the Calvin cycle (Chollet, 1973; Kagawa and Hatch, 1974). Partitioning of photosynthetic activities between M and BS cell types is mediated by cell-specific localization of multiple transcripts (Sawers et al., 2007) and proteins (Majeran et al., 2005). However, little is known about the transcriptional program regulating C_4 differentiation.

Previous studies have suggested that a small number of regulatory changes are sufficient to establish the C_4 syndrome (Ku et al., 1996). To date, localization of a limited number of transcripts has been shown to be mediated by *cis*-regulatory elements (Langdale et al., 1991; Schaffner and Sheen, 1991; Sheen, 1991; Schaffner and Sheen, 1992; Stockhaus et al., 1997). However, the discovery of a 'master switch' that will explain the thousands of genes with

cell-specific patterns of expression (Sawers et al., 2007) is unlikely (Edwards et al., 2001a). Rather, the accumulation of many of these transcripts may be mediated by changes that have resulted in novel cellular environments in the C_4 leaf that continue to control gene networks through pre-existing C_3 regulation. These factors could include differential sugar concentrations, protein complexes and gradients of small metabolites that influence M and BS cell identity.

Another factor that may influence the differentiation process is redox poise. In the leaf blade, M cells contain both PSII and PSI activities and perform linear photosynthetic electron transport (PET). In contrast, BS cells lack detectable levels of functional PSII and are believed to be restricted to cyclic electron transport (Gregory et al., 1979; Ghirardi and Melis, 1983; Romanowska et al., 2006). As a result, proper functioning of M and BS cells is dependent on the intercellular transfer of photosynthetically-derived reducing equivalents from M to BS cells. Specifically, NADPH generated during linear PET in M cells is exported for Calvin cycle activity in BS cells (Edwards and Walker, 1983). Thus, these differences in photochemistry lead to distinct redox profiles in the cellular environments of M and BS cells.

The characterization of mutants that are selectively disrupted in either M or BS cell photosynthetic differentiation may prove useful in understanding the networks that drive this process. For instance, *bundle sheath defective2* (*bsd2)* lacks Rubisco (Roth et al., 1996; Brutnell et al., 1999), and the mutant BS cells cannot perform the Calvin cycle (Smith et al., 1998). Consequently, the M cell linear PET chain is likely to be more reduced than in wild-type (WT) because it lacks an electron sink. Conversely, M cell defective mutants that lack PSII are unable to generate electron flow and likely result in overly

oxidized linear PET chains. Additionally, both of these mutant classes will fail to accumulate soluble sugars due to the absence of photosynthesis. Thus, mutations that disrupt the cellular environments of M and BS cells may provide useful tools for probing the differentiation process.

Several maize mutants have been reported with defects in PSII function including *hcf3, hcf19G* and *hcf19YG* (Leto and Miles, 1980). However, the molecular lesions associated with these PSII-defective mutants have yet to be determined. In this study, we identify an *Ac*-induced maize mutant that lacks PSII activity. Cloning and characterization of this gene indicates that it is a homologue of *Hcf136*, which is necessary for PSII assembly or stability (Meurer et al., 1998; Plucken et al., 2002). In WT plants, Zm *Hcf136* transcript accumulation is predominantly confined to M cells, and proteomic analysis of *hcf136* total leaf tissue shows that monomeric and dimeric PSII complexes do not accumulate. Interestingly, the plastid-encoded *psbB-psbT-psbH-petB-petD* polycistron is misprocessed in the mutant specifically in M cells. Microarray analysis reveals that M and BS cell transcript pools are altered by the *hcf136* mutation. The loss of PSII leads to a disruption in spatial regulation of typically BS-enriched genes and an increase in the cellular specificity of typically M-enriched genes. Additionally, data from the protein and transcript profiles do not always correspond, suggesting that post-transcriptional/translational controls are also involved in C_4 differentiation.

RESULTS

Ac tagged Zm *hcf136* is seedling lethal

The Zm *hcf136* mutant was first identified in sand bench screens of an *Ac*-mutagenized population as a recessive high chlorophyll fluorescence (hcf)

seedling lethal mutant (see Materials and Methods). DNA blot analysis identified a 2.5 kb *Eco*RI fragment containing an *Ac* insertion that co-segregated with the mutant phenotype. Inverse PCR with primers designed to *Ac* (Kolkman et al., 2005) was used to amplify 265 bp of DNA flanking the *Ac* insertion. Initial BLAST searches revealed that this fragment has significant similarity to the *Arabidopsis thaliana* gene *HCF136*, suggesting the *Ac* inserted into an exon of a maize *Hcf136* homologue. The *hcf136* mutant displays somatic instability consistent with an active transposable element insertion. In *Arabidopsis*, HCF136 is a lumenal protein that is specifically required for the assembly or stability of PSII (Meurer et al., 1998; Plucken et al., 2002). In maize, PSII accumulation is preferentially localized to mature M chloroplasts (Edwards and Walker, 1983; Schuster et al., 1985; Majeran et al., 2005).

To identify full-length maize coding sequences for *Hcf136*, the 265 bp flanking the *Ac* was used to search available genomic and EST databases, and a nearly full-length pseudomolecule of *Hcf136* transcript was assembled. To confirm the cloning of *Hcf136* and recover non-coding sequences associated with the *Hcf136* gene, we exploited the somatic instability of an active *Ac* allele to selectively amplify sequences flanking the *Ac* insertion in Zm *Hcf136*. By utilizing a genome walking technique known as '*Ac* casting' (Singh et al., 2003), we were able to recover additional sequence upstream and downstream of the original *Ac* insertion site. PCR reactions performed using gene-specific and *Ac* end primers resulted in the amplification of 2530 bp of genomic sequence flanking the *Ac* insertion, including 278 bp upstream of the start of translation (see Materials and Methods). Exon-intron boundaries were defined using reverse-transcriptase PCR as described in Materials and Methods and a schematic of the gene is shown in Figure 2.1A. The *Ac* element

Figure 2.1. Sequence analysis of the Zm *Hcf136* homologue. (A) The *Ac* element, shown as an arrow, is inserted in the sixth exon of Zm *Hcf136* between bp 1151 and 1152. Exons are represented by grey boxes and introns by solid lines. (B) Protein alignment of HCF136 homologues from *Zea mays*, *Sorghum bicolor*, *Oryza sativa*, *Arabidopsis thaliana*, *Guillardia theta* and *Synechocystis* sp. PCC 6803. Residues identical in at least three sequences are shaded black. Predicted mature start site of *A. thaliana* homologue is indicated by black arrow.

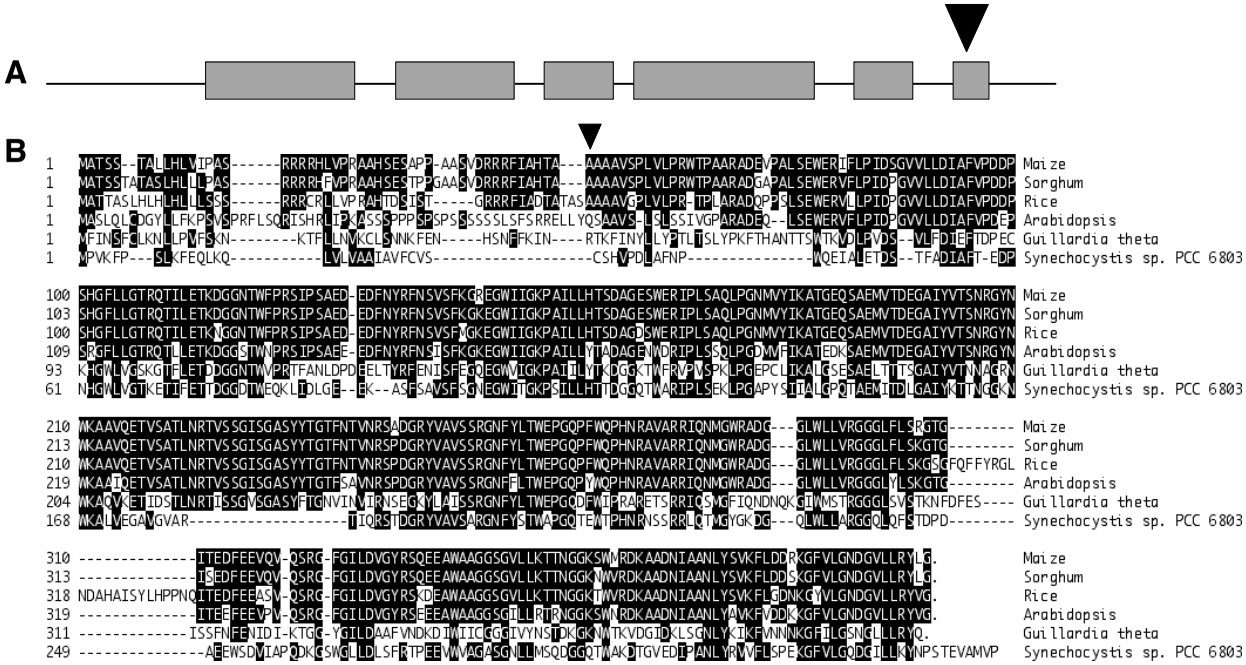
A
B
Maize
Sorghum
Rice
Arabidopsis
Guillardia theta
Synechocystis sp. PCC 6803

is oriented in the 3′ to 5′ direction relative to the start of transcription of *Hcf136* and is inserted in the sixth exon between bp 1151 and 1152 of the coding sequence. Rather than leading to a truncated protein, this orientation is predicted to produce a hybrid *hcf136-Ac* transcript that is likely unstable and degraded. A Zm *Hcf136*-specific probe was used to map the locus to the short arm of chromosome 1 (Bin 1.01) using the IBM recombinant inbred mapping population (Lee et al., 2002).

HCF136 proteins are highly conserved

As shown in Figure 2.1B, HCF136 homologues are highly similar across monocots, dicots, algae, and cyanobacterial species. TargetP predicts that Zm HCF136 is chloroplast-localized with a 25 amino acid transit peptide (Emanuelsson et al., 2000). When the predicted N-terminal transit peptide is excluded from sequence comparisons, At HCF136 and Zm HCF136 share 87% identity or 96% similarity across their entire length. Studies in *Arabidopsis* have suggested that HCF136 interacts directly with the PSII reaction core proteins D2 and Cyt b_{559} at the lumenal side of the thylakoid membrane (Plucken et al., 2002). Sorghum and maize HCF136 proteins are 96% identical, including the transit peptide. HCF136 from both the alga *Guillardia theta* and the cyanobacterium *Synechocystis* sp. PCC 6803 are 43% identical to maize. This high degree of sequence similarity between divergent species suggests a conserved and ancestral function for the HCF136 protein.

Loss of HCF136 affects PSII function and grana formation

Using *in vivo* fluorescence induction curves, we examined the functional status of PSII in *hcf136* leaves (see Materials and Methods). Mutant seedlings

displayed high chlorophyll fluorescence but no variable fluorescence, consistent with the absence of PSII activity (*hcf136* Fv/Fm = 0; WT = 0.8). Light microscopy of cross sections of WT and mutant leaf tissue revealed smaller chloroplasts in both M and BS cells of *hcf136* (Figure 2.2). Plastid ultrastructure was examined in greater detail using transmission electron microscopy (Figure 2.3). In the *hcf136* mutant, grana are absent or display aberrant ultrastructure in M plastids (Figure 2.3B). In contrast, plastid ultrastructure in *hcf136* BS cells appears normal (Figure 2.3D). These results are consistent with the prediction that the primary defect in Zm *hcf136* is a disruption in PSII assembly and accumulation.

Zm *Hcf136* transcripts accumulate preferentially in M cells

To determine whether Zm *Hcf136* transcript accumulation is M cell-specific, RNA blot analysis of several cell types and tissues was performed using an *Hcf136*-specific probe (Figure 2.4). RNA was isolated from light grown WT M cell protoplasts, BS strands, total leaf tissue, total *hcf136* mutant leaf tissue, and total leaf tissue from WT dark grown plants. To control for changes in gene expression due to M cell protoplast isolation, RNA was also extracted from total WT light grown tissue that was stress-treated by a mock protoplast digestion (see Materials and Methods). The RNA samples were hybridized with probes derived from the cell-specific markers *Pepc* and *Rbcs*, which accumulate preferentially in M and BS cell types, respectively (Sheen and Bogorad, 1987; Langdale et al., 1988a). As shown in Figure 2.4B, there is little cross-contamination in our cell preparations, and *Hcf136* transcripts clearly accumulate to higher levels in M relative to BS cells (Figure 2.4A). Additionally, *Hcf136* transcript accumulates in the dark but is more abundant

Figure 2.2. Light micrographs of 1 µm thick cross sections from the leaf blade tips of wild-type (A) and *hcf136* (B) at 400X magnification. Sections were cut by Shannon Caldwell and Anita Aluisio at the Cornell Integrated Microscopy Center (Veterinary Medical Center, Cornell University).


A


B

Figure 2.3. Plastid ultrastructure in second leaf tip of *hcf136* mutant and wild-type (WT) seedlings. (A) to (D) Transmission electron micrographs from seedlings grown under 80 µmol s^{-1} m^{-2} light in 16 h days at 50% humidity. Mesophyll plastids of WT (A) and *hcf136* mutants (B), bundle sheath plastids of WT (C) and *hcf136* mutants (D). Images by Shannon Caldwell and Anita Aluisio at the Cornell Integrated Microscopy Center.

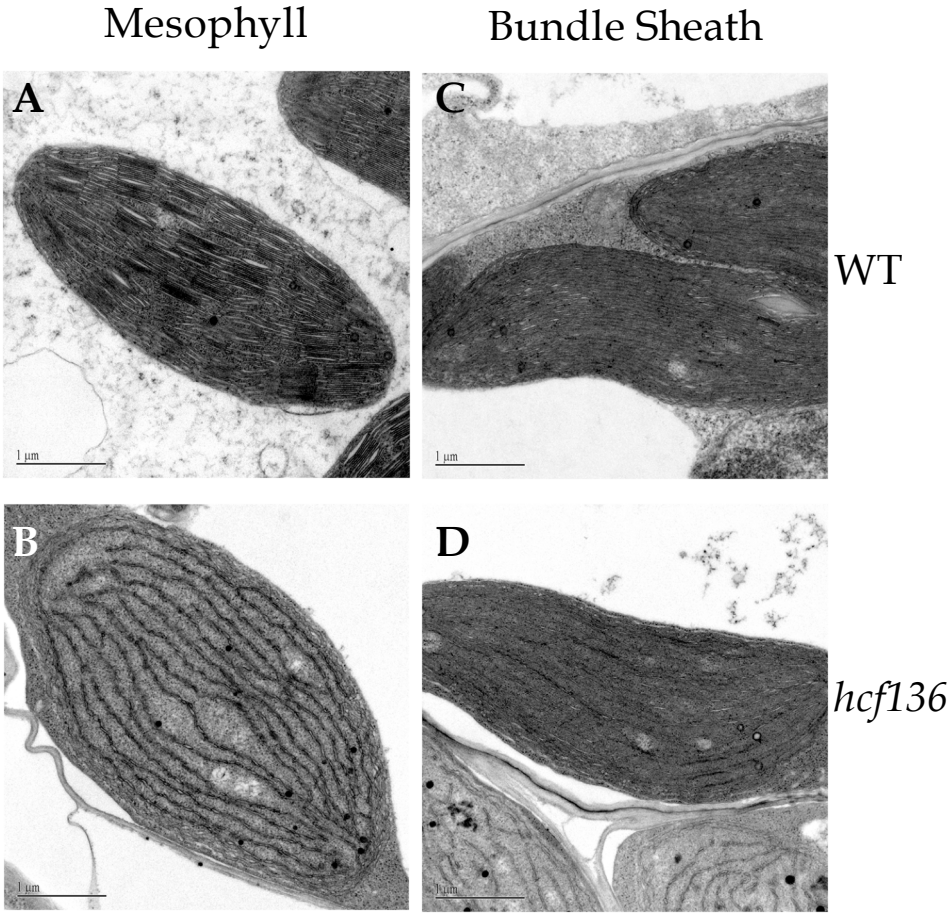
Mesophyll
Bundle Sheath
A
C
WT
B
D
hcf136
1 µm

Figure 2.4. RNA blot analysis of *Hcf136* transcript accumulation. (A) and (B) Approximately 5 µg of total RNA was fractionated on 1.5% agarose gels, transferred to nitrocellulose membrane and hybridized to radiolabelled fragments of *Hcf136* (A), *Pepc* (B), and *Rbcs* (B). Ethidium bromide-stained (Etbr) 18S rRNA is shown as a loading control.

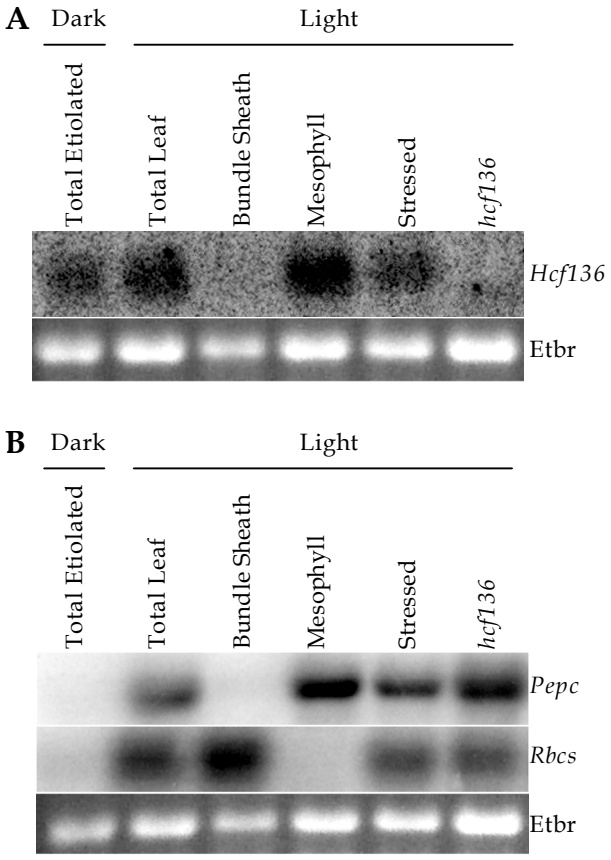
A
Dark
Light
Total Etiolated
Total Leaf
Bundle Sheath
Mesophyll
Stressed
hcf136
Hcf136
Etbr
B
Dark
Light
Total Etiolated
Total Leaf
Bundle Sheath
Mesophyll
Stressed
hcf136
Pepc
Rbcs
Etbr

in light grown tissues.

The *psbB-psbH-psbT-petB-petD* polycistron is misprocessed in M cells

When analyzing the mutant for changes in PSII transcript regulation, we unexpectedly observed a defect in the processing/stability of the *psbB-psbH-psbT-petB-petD* polycistron (Figure 2.5A). Components of PSII (*psbB*, *psbH*, *psbN* and *psbT*) and Cyt b_6f (*petB* and *petD*) are encoded by this polycistron, which is processed into many overlapping RNAs that are capable of directing protein synthesis (Barkan, 1988). As seen in Figure 2.5B, band 3 accumulates to much lower levels in the mutant leaf RNA, indicating a processing defect of the *petB* intron in *hcf136*. In addition, a fourth band (shown by asterisk) aberrantly accumulates in mutant M leaf tissue (Figure 2.5C). In contrast, the polycistron is processed similarly in mutant and WT BS cells. No processing defects were detected in *hcf136* mutants for other polycistronic transcripts examined including those encoding the core of PSII (*psbC*, *psbD*), and the group II intron family to which *psbB-psbH-psbT-petB-petD* belongs (*psaAB*, *atpF/H*) (Rock et al., 1987; Cushman et al., 1988; Kuck, 1989; Kim and Hollingsworth, 1993) (Figure 2.6). Since a processing defect was only detected in the *psbB-psbH-psbT-petB-petD* polycistron, these findings suggest that a disruption in HCF136 function specifically affects *psbB-psbH-psbT-petB-petD* processing in M cells.

Zm *hcf136* lacks HCF136 and PSII proteins

To examine the accumulation and localization of Zm HCF136, the profiles of WT and *hcf136* stroma-enriched and thylakoid peripheral and lumenal proteins were compared by 2-dimensional (2D) gel electrophoresis

Figure 2.5. *psbB-psbT-psbH-petB-petD* processing in *hcf136.* (A) Schematic shows polycistronic organization to scale with probe locations marked above the gene by a thick black bar. Genes that are encoded on the plus strand are labelled above their corresponding box, and the minus strand gene is labelled below. Exons and introns of *petB* and *petD* are also labelled below their corresponding gene. Numbered lines represent bands in the blots shown in (B) and (C). (B) RNA from total leaf tissue of wild-type (WT) and *hcf136* was hybridized to fragments of *psbB, psbH/N,* and *petD*. (C) RNA from separated mesophyll (M) and bundle sheath (BS) cells from WT and *hcf136* was hybridized to *psbH/N*. Processed fragments shown in (A) and (B) are marked by numbered arrows and an unidentified band is marked by an asterisk.

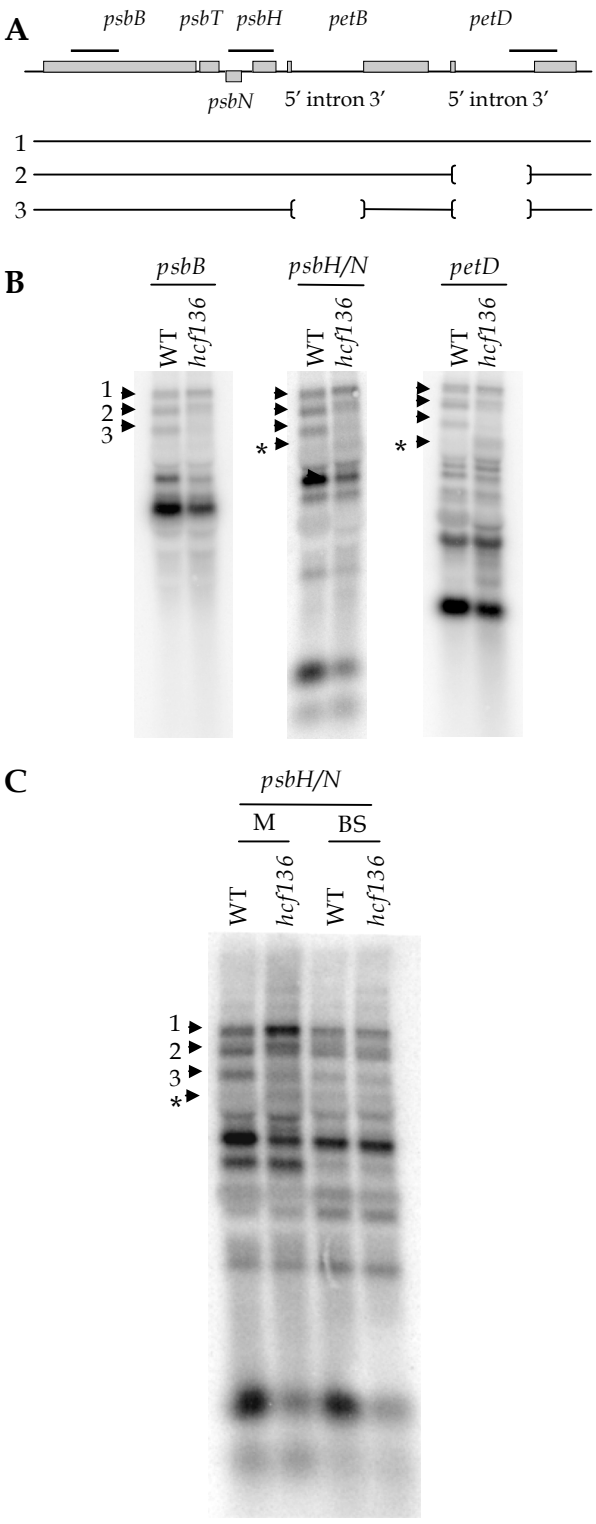
A
psbB
psbT
psbH
petB
petD
psbN
5′ intron 3′
5′ intron 3′
1
2
3
B
psbB
psbH/N
petD
WT
hcf136
WT
hcf136
WT
hcf136
1
2
3
*
*
C
psbH/N
M
BS
WT
hcf136
WT
hcf136
1
2
3
*

Figure 2.6. RNA blot analysis of polycistronic transcripts. (A) to (D) Total RNA from wild-type (WT) and *hcf136* leaf tissue were hybridized to gene-specific fragments of *psbC* (A), *psbD* (B), *atpF/H* (C) and *psaAB* (D).

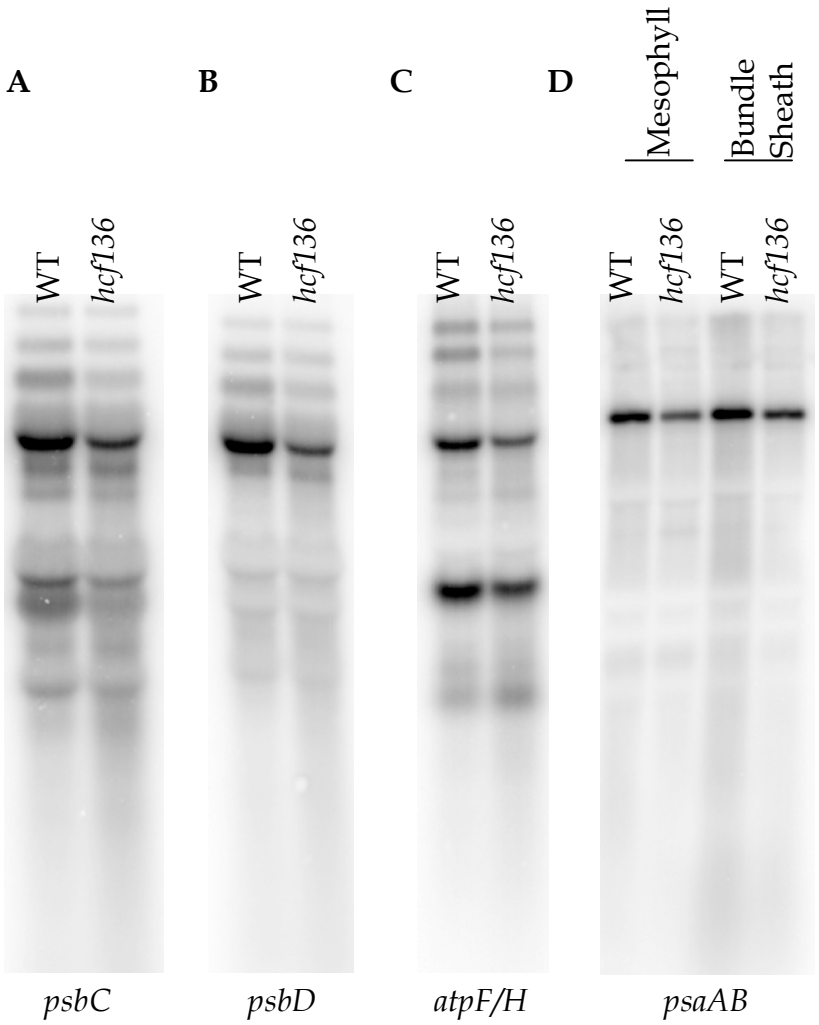
A
B
C
D
Mesophyll
Bundle Sheath
WT
hcf136
WT
hcf136
WT
hcf136
WT
hcf136
WT
hcf136
psbC
psbD
atpF/H
psaAB

with immobilized pH gradient (IPG) strips in the first dimension and SDS-PAGE in the second dimension. A single spot was identified in Sypro Ruby-stained 2D gels as a spot that is present in plastid protein extracts of WT plants but absent in *hcf136* mutants (Figure 2.7). This spot was excised, trypsin-digested and analyzed by electrospray tandem mass spectrometry (ESI-MS/MS) and identified as HCF136, confirming the identity of the *Ac*-tagged gene (TC296744; http://ppdb.tc.cornell.edu/).

To identify plastid-localized proteins that differentially accumulate in the *hcf136* mutant, thylakoid membranes were isolated, sub-fractionated into membrane and soluble components, and separated by 1D-SDS-PAGE (Figure 2.8). Strong differential accumulation was observed for a number of bands in the membrane fractions but not in the soluble fraction. Eight major bands showing differential accumulation were identified by peptide mass finger printing (PMF) using a MALDI-TOF mass spectrometer as FtsH1 (band 1, TC292243), CP47 (band 2, NP_043049.1), OEC33-like (band 3, TC279249), PSII-D2 (band 4, NP_043009.1), LHCII-1 (band 5, TC286614), PPDK (band 6, TC286559), cpHSP70 (band 7, TC293193), and RBCS (band 8, TC286731). These identifications likely represent the most abundant protein in the band. In *hcf136*, FtsH1 metalloprotease accumulation was reduced, and the CP47, OEC33-like, and D2 subunits of PSII were absent or dramatically reduced. A slight reduction in the accumulation of the major LHCII-1 band was observed likely due to the absence of accumulation of its interacting PSII complex. PPDK, cpHSP70, and RBCS proteins had increased accumulation in the *hcf136* membrane fraction but no differential accumulation in the soluble fraction, suggesting that these proteins interact more strongly with thylakoid membranes in plastids that lack PSII or grana. It is unlikely that a treatment

Figure 2.7. A comparison of 2-dimensional electrophoresis (2-DE) gels from wild-type (WT) and *hcf136* mutant tissues. Purified stroma enriched (A) and thylakoid peripheral and lumenal protein fractions (B) (200 μg of protein) were separated based on isoelectric point on immobilized pH gradient (IPG) strips, with a linear pH gradient from 4 to 7. Focused IPG strips were reduced and alkylated, and proteins separated by SDS-PAGE in second dimension. Resulting 2-DE gels were stained with the fluorescent dye Sypro Ruby and images were acquired with exposure times that minimized saturation. A similar spot pattern is observed between WT and *hcf136* extracts, with few differentially accumulating spots. One spot (indicated by arrow) was present in WT fractions and absent in the *hcf136* mutant. The white rectangle indicates the expected area for this spot on *hcf136* gels. This spot was picked, digested with Trypsin and its peptide composition analyzed by ESI-MS/MS. Mass spectra data were searched against the TIGR maize EST assembly (ZmGI v16 supplemented with maize chloroplast and mitochondria sequences), indicating this spot contains the HCF136 photosystem II assembly factor (TC296744).

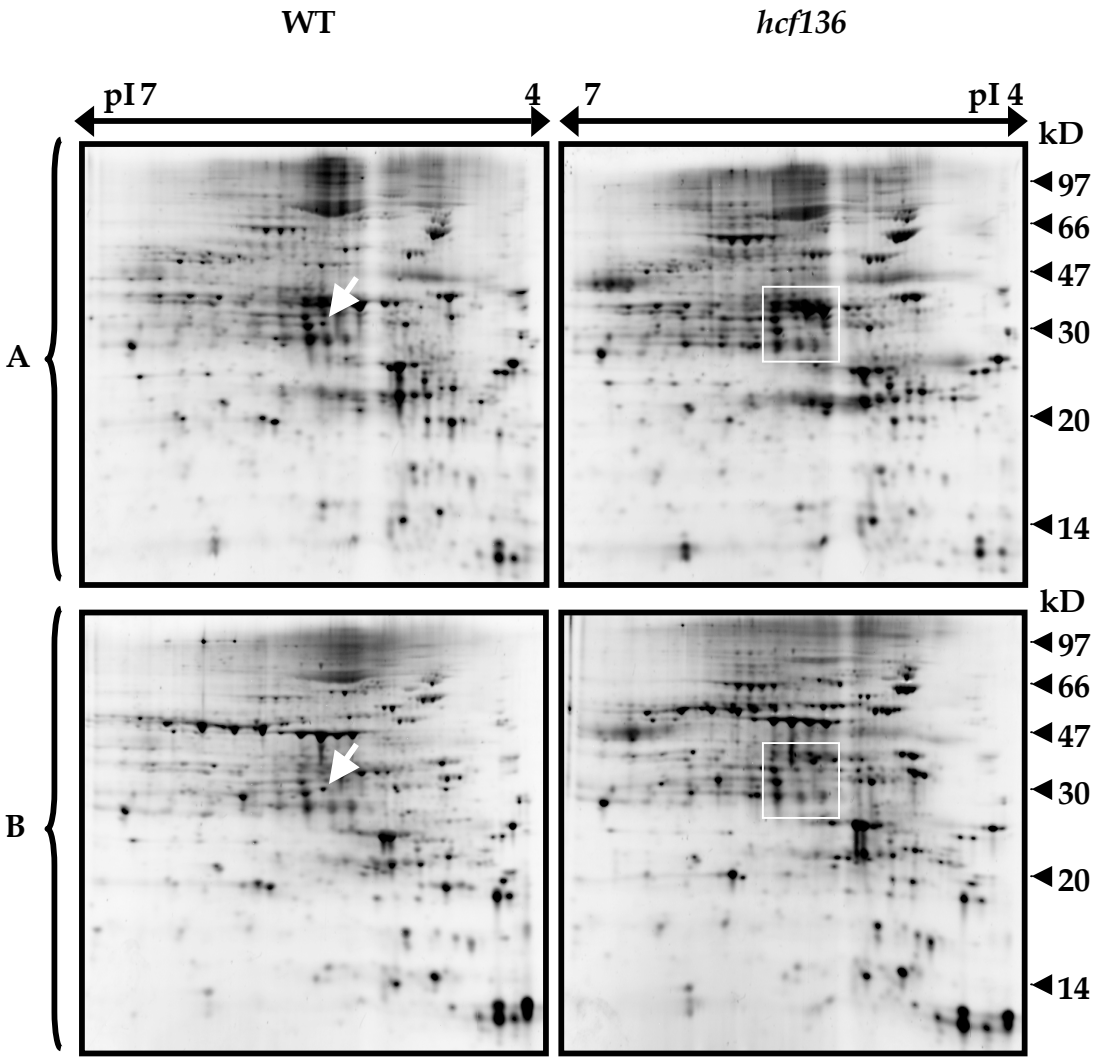
WT
hcf136
pI 7
4
7
pI 4
kD
97
66
47
30
20
14
A
B

Figure 2.8. 1D-SDS-PAGE analysis of *hcf136* mutant. Electrophoretic mobility pattern of wild-type (WT) and *hcf136* proteins obtained by SDS-PAGE (Tricine 12%) and stained with Sypro Ruby fluorescent dye. Total thylakoid membrane vesicles were isolated on Percoll cushions and then treated with a Dounce homogenizer followed by differential ultracentrifugation to collect membrane and soluble fractions. Bands displaying strong differential accumulation were excised and proteins digested and analyzed by MALDI-TOF MS PMF. Identified proteins are: 1 FtsH1 (TC292243), 2 CP47 (NP_043049.1), 3 OEC33-like (TC279249), 4 PSII-D2 (NP_043009.1), 5 LHCII-1 (TC286614), 6 PPDK (TC286559), 7 cpHsp70 (TC293193), and 8 RBCS (TC286731). These proteins are labelled with numbered arrows. Protein markers in kDa are indicated on the right.

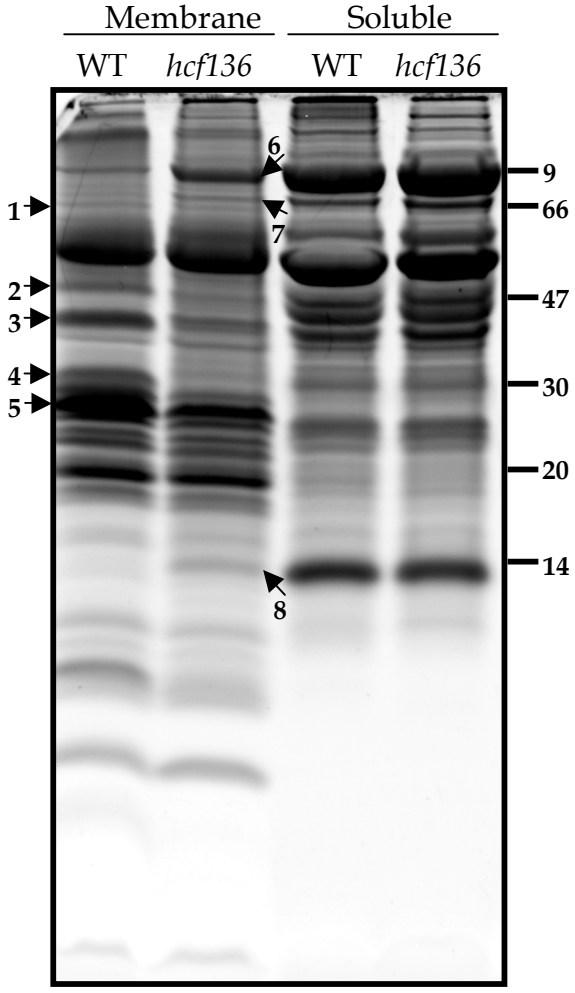
Membrane
Soluble
WT
hcf136
WT
hcf136
1
2
3
4
5
6
7
8
9
66
47
30
20
14

effect from thylakoid preparation accounts for this result since other abundant chloroplast soluble components are not found in the membrane fraction.

To improve resolution of the thylakoid proteome analysis and to determine the assembly state of the major photosynthetic complexes in WT and *hcf136*, thylakoids were solubilized with the non-ionic detergent n-dodecyl β-D-maltoside and analyzed by Blue Native (BN) gel electrophoresis followed by SDS-PAGE (2D-BN-SDS-PAGE) (Figure 2.9). Major photosynthetic complexes in WT and mutant tissues were identified by PMF analysis. In *hcf136*, PSII reaction center and core subunits are absent from thylakoid membranes, but there is no dramatic effect on the accumulation of PSI. The *hcf136* mutant also has a different oligomeric assembly state of the major light harvesting complex II (LHCII), which is present in a monomeric form rather than the trimeric form typical of WT thylakoids (Dekker and Boekema, 2005). This may be a consequence of the loss of its interaction partner, PSII core complex. Alternatively, the absence of membrane stacking may lead to increased accessibility to detergent and destabilization of LHC oligomers during membrane preparation. Other protein complexes, including ATP synthase and Cytochrome b_6f, accumulate to similar levels in both WT and mutant plastids.

Changes in protein accumulation do not correlate with RNA levels

To determine whether RNA level regulation is associated with the observed changes in protein accumulation, the relative abundance of several transcripts were measured by real-time quantitative PCR (qPCR) in separated M and BS cells (see Materials and Methods). Relative transcript levels were assayed using primer pairs specific to the following nuclear-encoded genes:

Figure 2.9. Blue-Native gel electrophoresis of thylakoid membranes from wild-type (WT) and *hcf136* mutants. Equivalent amounts of WT and *hcf136* thylakoid membranes (700 μg of protein) were solubilized with n-dodecyl β-D-maltoside and separated on native gels in the first dimension. Gel strips were reduced and alkylated in a solubilization buffer and separated by second dimension SDS-PAGE (Tricine 12%). Proteins were identified by in-gel digestion, followed by MALDI-TOF MS PMF. Protein complexes were identified as: I. PSI and PSII "supercomplexes", II. PSI and PSII dimer, III. partially assembled PSI, IV. PSII, ATP-synthase and cytochrome b_6f, V. partially assembled PSII, VI. and VII. LHCII. The *hcf136* mutant has additional complexes: Vb-VIb. LHCI-4 and VIIb. low molecular weight form of LHCII-1 complex. In the WT gel, black boxes indicate the different forms of PSII present in WT but absent in *hcf136*. In the *hcf136* gel, black boxes indicate changes in LHCI accumulation and in the assembly state of LHCII. Spot identities are as follows: 1. LHCI-3 (TC286618), 2. PsaD-2 PSI subunit II (TC293201, TC293200), 3. PsaD-2 PSI subunit II (TC293201, TC293200), 4. PsaF PSI subunit III (TC299208, TC299217, TC299206), 5. PsaE-2 PSI subunit IV (TC279867), 6. Non Identified, 7. Non Identified, 8. CF1β - *atpB* (TC279356) and CF1α - *atpA* (TC303520), 9. CP47 *psbB* (TC283413), 10. CF1g - *AtpC* (TC287102), 11. D1 *psbA* (TC290677), 12. Cytochrome b_6f Rieske Fe-S (TC286511), 13. non identified, 14. LHCII-1 (TC299123), 15. LHCII-1 (TC286602), 16. LHCII-1 (TC299123), 17. LHCII-3 (TC286603), 18. LHCI-4 (TC279557). Protein marker positions in kDa are indicated between the two gel images.

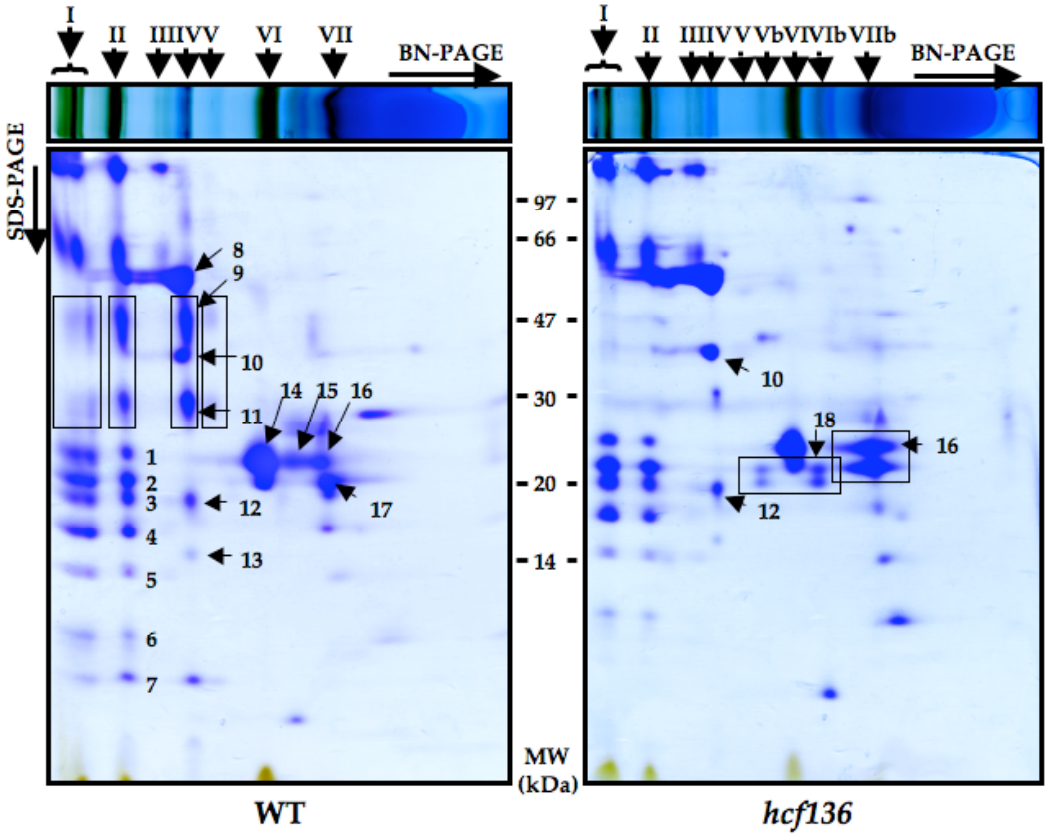
I
II
IIIIVV
VI
VII
BN-PAGE
SDS-PAGE
8
9
10
11
14
15
16
1
2
3
12
17
4
13
5
6
7
97
66
47
30
20
14
MW
(kDa)
WT
I
II
IIIIVV
VbVIVIb
VIIb
BN-PAGE
10
18
16
12
hcf136

Rbcs (TC286731), *Ppdk* (TC286559), *FtsH1* (TC292243), cp*Hsp70* (TC293193), *PsbO* OEC33 (TC279249), *Lhcb1* (TC286614), *Lhca3* (TC286618), *PsaD* (TC293201, TC293200), *PsaE* (TC279867), *PsaF* (TC299208, TC299217, TC299206), and *AtpC* (TC287102) (Table 2.1). The plastid-encoded genes *psbB* (NP_043049), *psbD* (NP_043009), and *psbE* (TC279867) were also assayed. A comparison of transcript levels in M and BS cells of *hcf136* and WT is shown in Figure 2.10. A value greater than one indicates transcripts were more abundant in the mutant than in WT, and a value less than one indicates transcript abundance was greater in the WT sibling. These data show that the observed disruption in plastid protein accumulation does not correspond to a general reduction in transcript accumulation.

Interestingly, the qPCR data does suggest that disrupting PSII activity can diminish or enhance the BS:M expression gradient of some genes. Nuclear-encoded *Rbcs* is BS-enriched (Sheen and Bogorad, 1986a; Langdale et al., 1988a), and plastid-encoded *psbB, psbD,* and *psbE* transcripts are M-enriched (Kubicki et al., 1994). However, *Rbcs* expression is higher in mutant M cells and lower in mutant BS cells, relative to WT and therefore is less differentially expressed in *hcf136*. In contrast, several genes are more differentially expressed in the mutant than in WT. For instance, *PsaD* is expressed at similar levels in WT M and BS cells (Sawers et al., 2007), but in *hcf136* this transcript is more abundant in M cells and less abundant in BS cells resulting in differential accumulation. Similarly, M cell enriched *PsbO* (Furumoto et al., 2000) and *Lhcb* transcripts (Sheen and Bogorad, 1986b) are more differentially expressed between M and BS cells of the *hcf136* mutant relative to WT.

Table 2.1. Primer sequences for SYBR Green real time quantitative PCR.

Gene	Protein	Proteomics TC number	Forward Primer	Reverse Primer
Rbcs-4	SSU	TC286731	ACT GTC GAT TCG TTG GGT GAG GAA	ATT AAA GTA TTG TCG GCG CCT CGG
Ppdk	PPDK	TC286559	CCG CCA AGT TGC TGA GAA AGT GTT	AGA AGA ATT CAG CCT GCT CCG CTA
FtsH1	FtsH1	TC292243	TGC TCC AAG CGA AGA AAG GCT AGA	TGT CTT GGC CAA AGA TCA CCT CCT
Hsp70-2	HSP70	TC293193	AGG AAT ACC ACA CTG CCA ACC TCA	TTC CAA CGG ACT TGT TGT CCC TGA
PsbO	OEC33	TC279249	AAA CGT ACA TGG AGG TGA AGG GCA	AGC TTC TTC ATC TGG TAC TTG CCG
Cab-M9	LHCII-1.5	TC286614	AGC TCA AGG TGA AGG AGC TCA AGA	ATA GGC CCA TGC GTT GTT GTT GAC
Lhca3	LHCI-3 - LHCI-680A CAB4	TC286618	AGC CTG CTG CCT GTA ACA ACA AAC	ACC ATG GTC ATG GCC TTA GGA GAA
PsaD	PsaD	TC293201, TC293200	TAA TCA CAC TTC ACG TAC GCC GCA	ACA TCT CAA ATC ATG CCA CCA CCG
PsaE	PsaE	TC279867	TTG GAC GAG GTC TCA GAG GTG AAA	GCA TGC AGC TTC ACA GCC TCA TTT
PsaF	PsaF	TC299208, TC299217, TC299206	ACG ACA AGG ACA TCG GCT ACT ACT	AAA GCC ATG TTT CCC ACG TAC GAC
AtpC	CF1c	TC287102	CAC AAA CGC AAC GGA GTT CTG TGT	GAC GTC TCA GTT GCG GCA AGA TTA
psbB	CP47	NP_043049	TGG AGT TAT GAA GGT GTG GCA GGT	TTT CCC GTC CGC TCA TCA CAG AAT
psbD	D2	NP_043009	CGT CAA TTT GAA CTT GCT CGG CCT	ACC AAC CAG ATT GTC CCA GTG GAT
psbE	Cyt b559	TC279867	ACC TTC CCT ATT CAT TGC GGG TTG	ACT CGT TTG GTC GAG GAC TTC CAA

Figure 2.10. Transcript abundance in mesophyll (M) and bundle sheath (BS) cells of *hcf136* mutant relative to wild-type (WT). Fold-change values greater than one correspond to greater transcript abundance in *hcf136* tissues relative to WT as measured by real time quantitative PCR. Means of three biological replicates and two technical replicates for each sample are shown with standard error estimates.

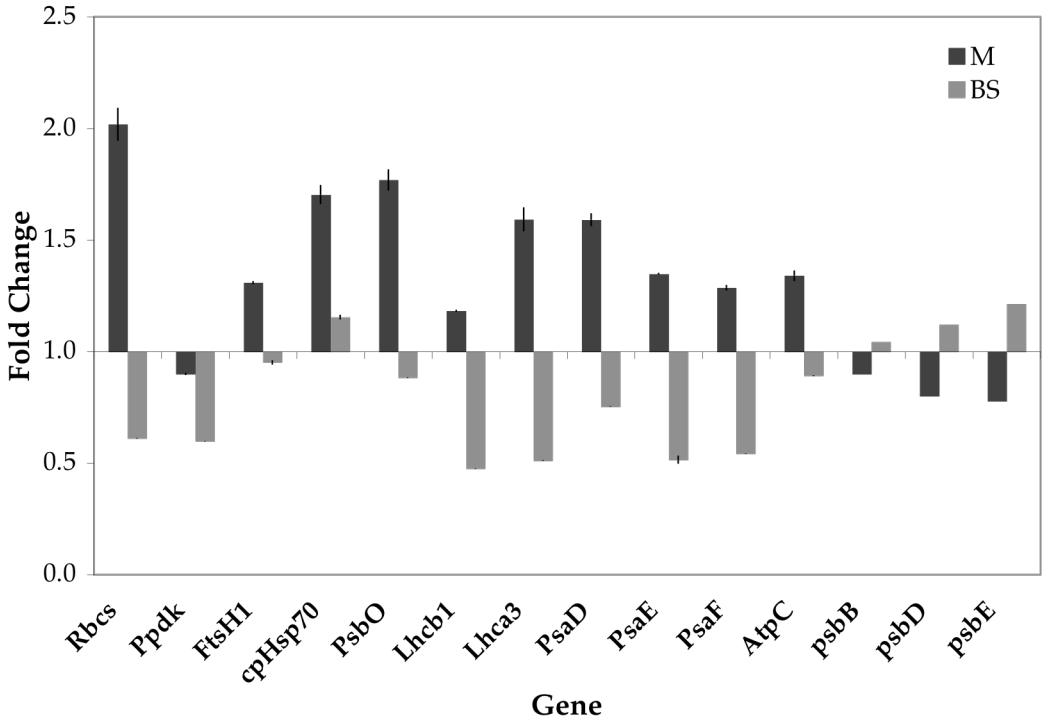
2.5
2.0
1.5
1.0
0.5
0.0
Fold Change
M
BS
Rbcs
Ppdk
FtsH1
cpHsp70
PsbO
Lhcb1
Lhca3
PsaD
PsaE
PsaF
AtpC
psbB
psbD
psbE
Gene

Loss of PSII leads to changes in C_4 spatial regulation

To further explore the disruption of PSII activity on gene expression, transcript profiles from separated M and BS cells were examined using two-label microarray analysis (see Materials and Methods). To avoid confounding treatment effects associated with direct comparisons of M and BS transcriptomes (Sawers et al., 2007), comparisons were only made using the same cell type across the *hcf136* and WT sibling genotypes. After normalization and filtering, 7377 and 8463 features were considered for further analysis from the M and BS experiments, respectively. These two data sets share 5670 common features as summarized in Figure 2.11A.

Using a false discovery rate (FDR) of 5%, we identified 2568 differentially expressed features between *hcf136* and WT in the M cell data set. When a more stringent 1% FDR cut-off is applied, 1078 features are differentially expressed, of which 162 have at least a two-fold change in expression and 773 are more abundant in the mutant relative to WT. In the BS experiment, 1669 features are differentially expressed between *hcf136* and WT at a 5% FDR and 586 at a 1% FDR. In the 1% FDR BS data set, 195 features change by at least two-fold relative to WT and 306 are more abundant in the mutant relative to WT. When the differentially expressed genes are compared at a 5% FDR between M and BS data sets, 573 features are identified that are common to both cell types (Figure 2.11B). This overlap is reduced to 147 features when significance is controlled at a 1% FDR (Figure 2.11C). Since only 14% or 9% (high and low FDR) of differentially expressed features are shared, these data suggest there is a cell-specific transcriptional response to the loss of PSII.

A comparison of our data to a previous study (Sawers et al., 2007)

Figure 2.11. Venn diagrams demonstrating unique expression profiles of *hcf136* mesophyll (M) and bundle sheath (BS) cells. (A) Total features detectable in M and BS cells. (B) Features differentially expressed in *hcf136* at a 5% false discovery rate (FDR). (C) Features differentially expressed in *hcf136* at a 1% FDR.

A

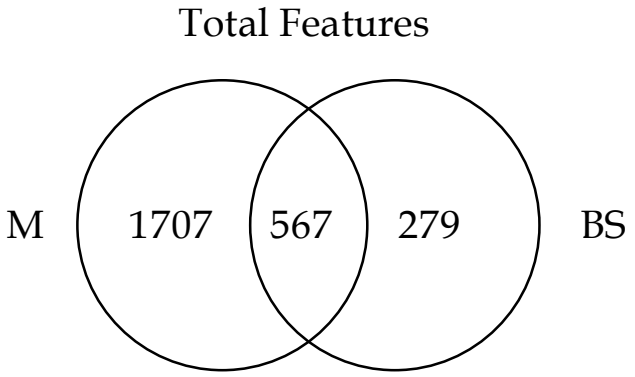
Total Features
M
1707
567
279
BS

B

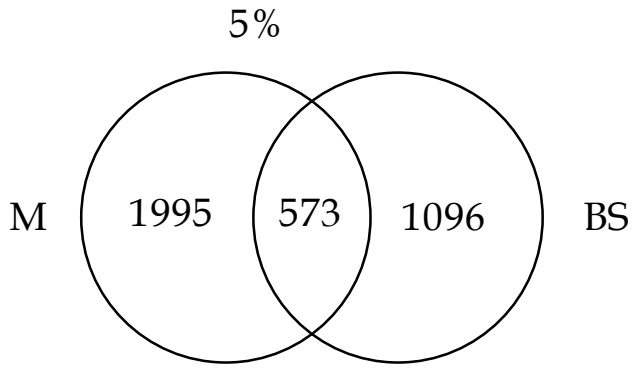
5%
M
1995
573
1096
BS

C

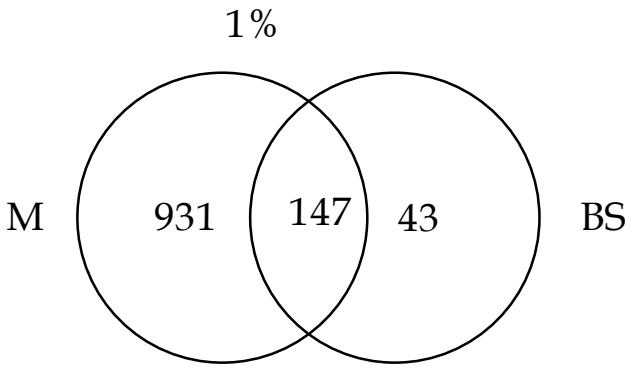
1%
M
931
147
43
BS

shows that BS:M ratios of 129 features that preferentially accumulate in M cells and 167 that preferentially accumulate in BS cells are altered in the *hcf136* mutant relative to WT. For example, *Phosphoenolpyruvate carboxykinase* (MZ00013532), which has a WT BS:M ratio of 2.82 and a predicted *hcf136* ratio of 1.39, is less differentially expressed in the mutant. Conversely, *Carbonic anhydrase* (MZ00042197), which has a BS:M ratio of 0.24 in WT and a predicted ratio of 0.18 in *hcf136*, is more differentially expressed in the *hcf136* mutant. Of the 129 M-enriched transcripts, 57% are more differentially expressed in the mutant relative to wild type (e.g. M:BS mutant > M:BS WT). Conversely, of the 167 BS-enriched transcripts, only 29% are more differentially expressed in the *hcf136* mutant. These results suggest that M and BS cells respond differently to a disruption in PSII function.

To verify the altered transcriptional profiles determined by microarray analysis, RNA blots were performed (Figure 2.12). Probes were designed to a number of plastid- and nuclear-encoded genes with highly abundant transcripts involved in photosynthesis that are differentially expressed between *hcf136* and WT at a 5% FDR in at least one cell type. From the M cell data, chloroplast-encoded *psaAB*, *rbcL*, *psbH, matK* and nuclear-encoded *Lhcb* were chosen for verification. From the BS data, chloroplast-encoded *rbcL* and *matK* plus nuclear-encoded *PsbS*, *Lhcb* and *Rbcs* were chosen for confirmation. As shown in Figure 2.12, RNA blot analysis confirmed the differential accumulation of these genes between WT and mutant plants. The expression change of *PsbS* in BS cells was at the limit of detection (Figure 2.12), but these data were confirmed using qPCR (Figure 2.13). Collectively, these data validate a subset of the microarray results indicating differential responses of M and BS cells to a loss of HCF136 function.

Figure 2.12. RNA blot analysis of differentially expressed genes. (A) to (C) RNA blots of separated mesophyll (M) and bundle sheath (BS) cells of *hcf136* and wild-type (WT) siblings were sequentially hybridized with radiolabelled gene fragments shown. Each blot was first probed with a cell specific marker to ensure isolation purity (*Me, Pepc, Rbcs)*. The nuclear [N] and chloroplast [C] encoded genes include *PsbS* [N], *matK* [C], *psaAB* [C], *rbcL* [C], *Lhcb* [N], and *psbH* [C]. Ethidium-bromide (Etbr) stained 18S RNA is shown as a loading control.

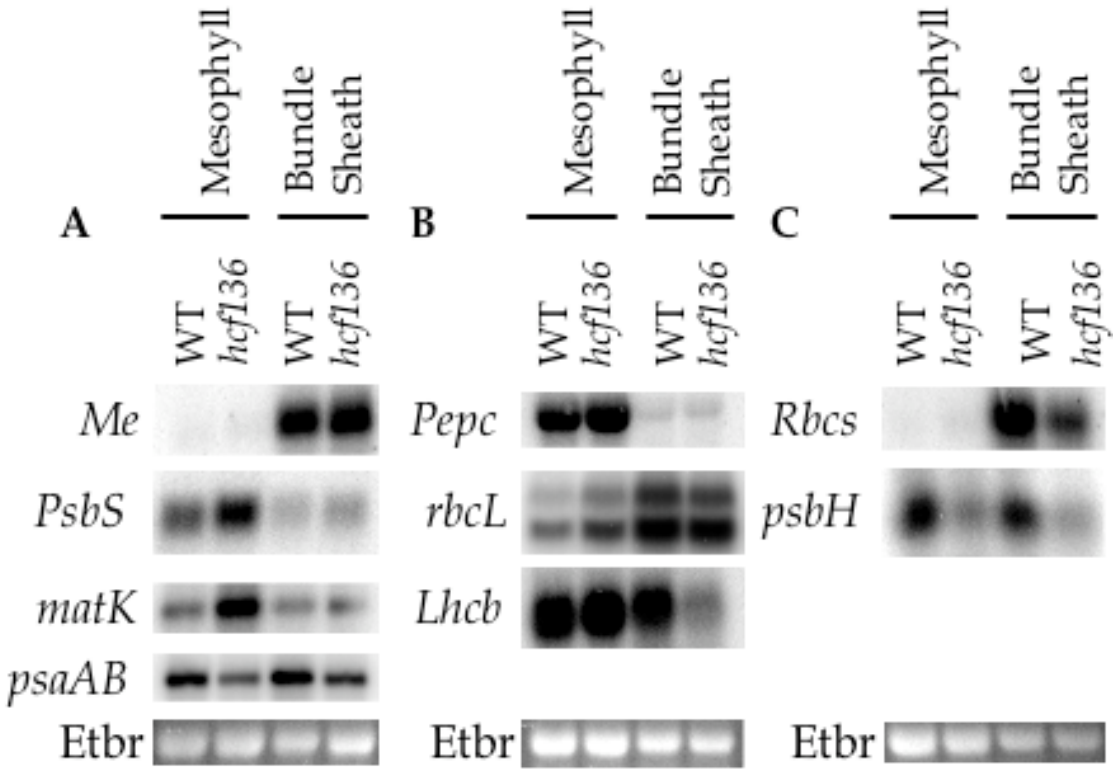
A
Mesophyll
Bundle Sheath
WT
hcf136
WT
hcf136
Me
PsbS
matK
psaAB
Etbr
B
Mesophyll
Bundle Sheath
WT
hcf136
WT
hcf136
Pepc
rbcL
Lhcb
Etbr
C
Mesophyll
Bundle Sheath
WT
hcf136
WT
hcf136
Rbcs
psbH
Etbr

Figure 2.13. Quantitative real-time PCR of relative transcript levels of *PsbS* between wild-type and *hcf136* within mesophyll (M) and bundle sheath (BS) cell types.

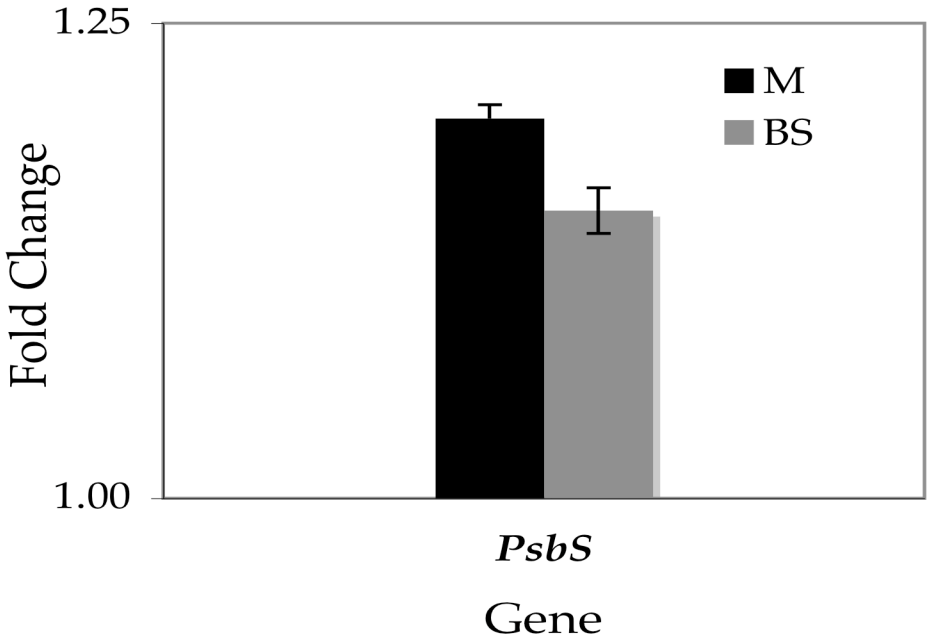
1.25
1.00
Fold Change
M
BS
PsbS
Gene

DISCUSSION

HCF136 function in maize

Using the transposable element *Ac* as a molecular tag, the Zm *Hcf136* gene was cloned and characterized. The pale green, seedling lethal Zm *hcf136* mutant displays reduced thylakoid stacking in M plastids, an absence of PSII complexes, and no detectable PSII reaction center functionality (Fv/Fm=0). These data are consistent with the previously assigned function of HCF136 as a PSII reaction center assembly or stability factor (Meurer et al., 1998; Plucken et al., 2002). In maize, PSII activity is largely restricted to the M cells resulting in a cell-specific defect in mutant leaf tissues.

Loss of PSII protein accumulation in *hcf136*

Although PSII reaction center and core proteins fail to accumulate to detectable levels in *hcf136*, the corresponding transcripts of both nuclear and chloroplast genes accumulate to near WT levels. This lack of correlation between proteome and transcriptome profiles is likely a consequence of protein degradation of unassembled PSII reaction center and core proteins in the chloroplast. In contrast, nuclear-encoded protein components of PSI (PsaD, E, F) and ATP synthase (CF1g - *AtpC*) accumulate to similar levels in mutant and WT tissues, but the corresponding transcripts accumulate to higher and lower levels in mutant M and BS plastids, respectively, relative to WT. Thus, the nuclear-plastid transcriptional networks in these two cell types respond selectively to a loss of PSII function.

Altered transcript patterns in *hcf136*

The microarray data revealed that while many features are detectable

in both M and BS cells of *hcf136* (5670), only 573 features are differentially expressed between WT and mutant and are shared between cell types at a 5% FDR and 147 at a 1% FDR. These data suggest that M and BS cells are responding differently to a perturbation in HCF136 function. Striking examples of these differences in regulation can be observed in transcripts encoded by the plastid genome at a 5% FDR. For instance, different sets of genes encoding PSII components respond in *hcf136* M and BS plastids. In mutant M plastids, *psbH, J, M,* and *N* are differentially expressed relative to WT, whereas in BS plastids *psbD, E, J,* and *K* show altered accumulation profiles. Also, three components of ATP synthase (*atpA, B, E)* and four components of NADH dehydrogenase (*ndhE, F, G, I*) are differentially expressed in M cells but not in the BS. Additionally, significant changes in *psaB, petA*, *petD, rpoA*, *rpoB*, and *infA* expression are only detected in M cell comparisons. In contrast, transcripts for *psaJ, rpoC2, atpI,* and *ndhJ* are differentially expressed solely in the BS.

Another striking trend in the M cell expression data is that nearly twice as many features are differentially expressed in M cells (2568) relative to the BS (1669) at a 5% FDR. This trend is most evident for plastid-encoded transcripts, where 57 genes are differentially expressed between WT and mutant in M chloroplasts and only 18 genes are differentially expressed in BS plastids. For example, out of 21 *rpl* and *rps* genes detected in both cell types, all 21 are differentially expressed in the M cells but only two of those 21 are differentially expressed in BS strands. In general, transcripts encoded by the plastid genome are more abundant in the mutant relative to WT when differentially expressed. Specifically, only *psbH*, *psaB, ndhJ, atpI, rps14,* and *rbcL* are less abundant in *hcf136* than in WT. Consequently, these data suggest that

pools of plastid mRNA, particularly in the M, are responding in concert and are either more stable or more highly expressed in the mutant. It is possible that the smaller global response in the BS may reflect its naturally PSII-depleted state.

A comparison of M and BS cell data sets shows that a greater percentage of differentially expressed features change by more than two-fold in BS relative to M cells at a 1% FDR (33% vs. 15%). This indicates that BS features are capable of a strong transcriptional response to the loss of PSII. For example, putative maize homologues of *Phosphatidylcholine acyltransferase* (MZ00018920), *Peroxidase* (MZ00015594), *U2 snRNP auxiliary factor* (MZ00006052), *H2B histone* (MZ00013518) and *BTH-induced ERF transcriptional factor1* (MZ00017004) are detected only in the BS cell experiment and increase in accumulation by more than two-fold. Similarly, *Phosphenolpyruvate carboxykinase* (MZ00013533), and a putative *Inositol 1,3,4-trisphosphate 5/6-kinase* (MZ00029181) decrease by more than two-fold in *hcf136* BS cells. In addition, some features are differentially expressed in both cell types, but the magnitude of the response is greater in the BS. For example, *Thylakoid formation1* (MZ00043318) increases 2.6-fold in the BS and only 1.9-fold in M cells. Similarly, *Cytochrome c* (MZ00013468) increases 2.3-fold in BS and 1.5-fold in M *hcf136* cells. Thus, M and BS cells are capable of independently regulating gene expression in response to a disruption of PSII.

We identified 296 features that were previously shown to differentially accumulate in BS and M cells (Sawers et al., 2007) and were misregulated in the *hcf136* mutant. As described above, the general trend is for less differential expression of BS-enriched features (118/167) and more differential expression of M-enriched transcripts (73/129) in *hcf136* relative to WT. Eighty-five of 118

BS-enriched features are less differentially expressed in *hcf136* due to an increase in expression in M cells. For example, *cytochrome c oxidase subunit 2* (MZ00034818) accumulates to similar levels in mutant BS cells as in WT but is more abundant in M cells of *hcf136*. This bias towards greater differential accumulation in *hcf136* M cells coincides with the observation that 72% of M cell features show increased expression in the *hcf136* mutant.

The role of cellular environment in C_4 differentiation

Current models propose that the evolution of C_4 biology from the basal C_3 state requires the recruitment of *cis*- and *trans*-acting regulatory elements to alter gene expression (Sage, 2004). However, a recent transcript profiling experiment indicates that nearly 18% of the leaf transcriptome is differentially expressed between M and BS cells (Sawers et al., 2007). Given the vast numbers of regulatory elements necessary to establish this magnitude of differential expression, we suggest that recruiting thousands of *cis*- and *trans*-acting elements to mediate transcriptional change is not a parsimonious explanation for how such a large percentage of the genome is spatially controlled. Rather, key regulatory changes may have resulted in novel M and BS cellular environments and in response extant C_3 networks may have been recruited during evolution of C_4 photosynthesis (Sheen, 1999; Hibberd and Quick, 2002), accounting for the majority of observed transcriptional changes. Factors that may drive M and BS gene expression include differential protein complex formation (e.g. OEC and PSII in M cell plastids), plastid redox status, and sugar and energy metabolite concentrations.

An example of misexpression due to a change in cellular environment may be the aberrant processing of the *psbB-psbH-psbT-petB-petD* polycistron

detailed in Figure 2.5. This defect is likely due to a change in the environment of M cell plastids that is associated with the loss of PSII (e.g. pH change, redox poise, thylakoid membrane structure). Although we have not ruled out a direct role for HCF136 in RNA metabolism, the *psbB* polycistron is aberrantly processed in several non-allelic *hcf* mutants including *hcf2*, *hcf38* and *hcf43* (Barkan et al., 1986). The less differentially expressed M- and BS-enriched features may also constitute a class of genes that are responding to a loss of C_4 cellular environments in the mutant. For instance, genes with BS to M expression ratios that are closer to 1 in *hcf136* relative to WT (e.g. *Pyruvate, orthophosphate dikinase* [MZ00007665] and *Phosphoenolpyruvate carboxykinase* [MZ00013532]) may represent a reversion to a more basal C_3 state (Langdale et al., 1988b). Together, these findings suggest that a general disruption of photosynthetic electron transport leads to altered processing of the *psbB* polycistron (Barkan et al., 1986) and deregulation of some spatially restricted transcripts.

Many nuclear genes respond to plastid-derived signals that are integrated through a common pathway in the chloroplast (Koussevitzky et al., 2007). In *Arabidopsis*, *genome uncoupled* (*gun)* mutants have been used to dissect plastid to nucleus retrograde signals. Susek et al. (1993) found that *Lhcb* and *Rbcs* expression is unchanged or elevated when *gun* mutants are treated with the herbicide Norflurazon. Using microarray analysis, Strand et al. (2003) identified 322 genes that are misregulated following Norflurazon treatments, 152 of which do not respond appropriately in at least one *gun* mutant. Recent studies of plastid-nuclear signaling in *Arabidopsis* have defined GUN1 as a central integrator of tetrapyrrole metabolism, redox and plastid gene expression state within the plastid. These multiple inputs are somehow

transduced into a signal that is transmitted to transcriptional regulators including ABI4 to regulate nuclear gene expression (Koussevitzky et al., 2007). It is possible that a disruption of PSII is similarly sensed by a plastid factor and this information is relayed to the nucleus. The slight but significant increase in the expression of many nuclear-encoded M-enriched transcripts in *hcf136* may be the consequence of the perturbation of PSII activity and loss (or reduction) of a plastid-derived signal that typically negatively regulates gene expression. Furthermore, the reduction in abundance of several transcripts in BS cells may be a secondary response to a loss of reducing equivalents or sugar metabolites rather than a direct response to the absence of PSII function.

In summary, the *hcf136* mutant has provided an opportunity to examine the effects of altered M and BS cellular environments on C_4 differentiation. The loss of PSII impacts M and BS protein composition, PET, redox poise, energy and sugar metabolite gradients. As a result, there is a general increase in RNA transcript accumulation in the M cell, and M- and BS-enriched features become more and less differentially expressed, respectively. Additionally, altering the BS cellular environment results in decreased transcript accumulation for a number of features, and this may reflect a shift to a more basal C_3 state in this cell-type.

MATERIALS AND METHODS

Identification of Zm *Hcf136*

The *Zea mays* (maize) homologue of *Arabidopsis thaliana Hcf136* was identified as part of a regional mutagenesis screen using *Ac/Ds* transposition in the W22 inbred line of maize. The mutant family JK03-77.24 was created by selecting transposition events from *bti00228*::*Ac* and subsequent screening of

self-pollinated populations (Kolkman et al., 2005).

DNA blot analysis was performed using an *Ac*-specific fragment (Ac900; (Kolkman et al., 2005) to identify an *Eco*RI restriction fragment length polymorphism (RFLP) that co-segregated with the mutant phenotype. This fragment was cloned using inverse PCR as previously described (Kolkman et al., 2005). BLAST sequence comparisons in available databases revealed similarity to HCF136 protein homologues. A Zm *Hcf136*-specific DNA fragment was mapped using RFLP analysis (Lee et al., 2002) with forward primer, JK03-77.24@FlAc900 (5′ CCGCCAATCTCTACTCCGTCAAGT) and reverse primer, *Hcf136* 3′UTR Common (5′ GGTTTTCAAGTTCCTAAGCAAGCAG).

Zm *Hcf136* sequence assembly

Ac casting was used to obtain genomic DNA sequence for the full Zm *Hcf136* gene (Singh et al., 2003). Nested PCR was performed using gene-specific primers in combination with *Ac* internal primers. The gene specific primers were 5′ *Ac* Casting 1 (5′ AGTCGATGGGCAGGAAGAT), 5′ *Ac* Casting 2 (5′ GCCGTCTTTCGTCTCCAGTA), 5′ *Ac* Casting 3 (5′ TCTGCTCCCCAGTAGCTTTT), 5′ *Ac* Casting 4 (5′ ACCGCTAATGCCACTTGAAA), and GC-HCF136 Common Exon (5′ AAAGTCCACCGTCCGCTCTC). Downstream primers were 3′ *Ac* Casting 1 (5′ GATGCATGTGCTGCTTGC), 3′ *Ac* Casting 2 (5′ GCGTGTTGCTTCGGTATCTT), and GC-HCF136 3'UTR Common (5′ CTGCTTGCTTAGGAACTTGAAAACC). PCR products were gel purified using QiaEXII (Qiagen, www.qiagen.com), cloned into pGEM (Promega, www.promega.com) or TOPO vectors (Invitrogen, www.invitrogen.com).

Plasmids were purified using the QIAprep Spin Miniprep Kit (Qiagen) according to manufacturer's recommendations. The DNA was sequenced as previously described (Singh et al., 2003).

Plant growth conditions

Plants were grown in 16 h days and constant 28°C under low light conditions of 80 μmol s^{-1} m^{-2} for fluorescence, electron microscopy and protein analyses and 40 μmol s^{-1} m^{-2} for all other experiments. Etiolated seedlings were grown in darkness at 28°C until their light-grown siblings were at the third leaf emerging stage. Mutants were identified from segregating families, and near-isogenic comparisons made with phenotypically WT siblings.

Fluorescence measurements

In vivo fluorescence induction curves for Fv/Fm were obtained at room temperature from the second leaf tip of seedlings at the third leaf emerging stage of development using an actinic light source and bright saturating pulse as previously described (Maxwell and Johnson, 2000). The leaf area assayed was dark adapted for at least 15 min prior to illumination. Fv/Fm measurements were obtained with a modulated fluorescence apparatus (model number FMS2; Hansatech Instruments, www.hansatech-instruments.com).

Electron microscopy

Electron microscopy was performed on WT and mutant plants at the third leaf emerging stage of development. Tips of the second leaves of 10-day-

old WT and mutant seedlings were harvested in the morning to deplete overnight starch reserves. Samples were fixed for 0.5 h at room temperature and 1.5 h at 4°C in 2.5% glutaraldehyde in 0.1 M sodium cacodylate, pH 6.8. The samples were rinsed at 4°C in 0.1 M sodium cacodylate buffer, pH 6.8, fixed in 1% osmium tetroxide, and rinsed in 0.1 M sodium cacodylate buffer, pH 6.8. Samples were dehydrated in a graded ethanol series then infiltrated with Spurr's resin. Sections were cut on a Reichert OmU2 Ultramicrotome and contrasted with uranyl acetate and lead citrate. The sections were viewed on a Tecnai 12 Biotwin transmission electron microscope (FEI Corporation, www.feicompany.com). Digital images were acquired using a Gatan Multiscan Camera, Model 791 (Gatan, www.gatan.com).

Cell preparation

M protoplasts, BS strands and the control stressed total tissue were prepared as previously described with a slight modification; rather than using second and third leaves, only second leaf blades were used (Markelz et al., 2003).

RNA isolation and blot analysis

Total RNA was isolated and analyzed by RNA blot as previously described (Sheehan et al., 2004). Leaf tissue from light-grown plants was harvested when the third leaf emerged. Dark-grown seedling tissue was harvested above the mesocotyl on the same day. Cell-specific markers were assayed to monitor the integrity of the M and BS preparations (*Pepc, Rbcs, Me*). Approximately, 5 µg of RNA was loaded for the initial analysis of *Hcf136* transcript accumulation (Figure 2.4). All other gel blots were prepared using

10 µg of RNA. Ethidium bromide staining of the 18S rRNA was used as a loading control.

DNA probes for this study's RNA blots include: *Hcf136, Pepc, Rbcs, Me, Lhcb-m7, rbcL, PsbS, matK, psaAB, psbH, petD, psbB, psbD, petB, psbA, psbC,* and *atpF/H*. The *Hcf136* probe was a 648 bp fragment at the 3' end of the gene made using the forward primer *Hcf136* Common Exon (5' GAGAGCGGACGGTGGACTTT) and reverse primer *Hcf136* 3'UTR Common (5' GGTTTTCAAGTTCCTAAGCAAGCAG). The *rbcL* probe was amplified from genomic maize DNA using the primers 5' GCAGTAGCTGCGGAATCTTCTACT and 5' GGTGAATGTGAAGAAGTAGGCCGT. *PsbS* was amplified using 5' TCTCCATCATCGGCGAGATCATCA and 5' TACAAGCAGACAACCCAACG. Other fragments were as previously described (Roth et al., 1996) or were generated using gene-specific primers to published maize plastid sequences. DNA probes were generated by PCR using GoTaq Green Master Mix (Promega), gel purified with QiaEXII, and radiolabelled according to Sheehan et al. (2004).

Protein characterization of Zm *hcf136*

Plants were grown as described above and tissue harvested for 2D-IPG-SDS-PAGE when the third leaf was emerging and for 2D-BN-SDS-PAGE and 1D-SDS-PAGE when the fifth leaf was emerging. Proteins were extracted from whole seedlings for 2D-IPG-SDS-PAGE and from apical regions about 4 cm from the tips of third and fourth leaves for other PAGE experiments. The total leaf microsomal fraction was isolated in grinding buffer (350 mM sorbitol, 50 mM Hepes-KOH pH 8, 2 mM EDTA, 5 mM ascorbic acid, 5 mM L-

cystein) in a Warring blender at half speed, followed by Miracloth filtration and low speed centrifugation (1000 g). The thylakoid membrane fraction was purified from the microsomal pellet on discontinuous Percoll gradients as previously described (Friso et al., 2004). Thylakoid membrane vesicles were treated with a Dounce homogenizer followed by differential ultracentrifugation (100 000 g) to collect membrane and soluble fractions. Protein concentrations were determined with the bicinchoninic acid (BCA) assay (Smith et al., 1985).

For 1D-SDS-PAGE separation, proteins were equilibrated with SDS (0.2%), Na_2CO_3 (100 mM), DTT (100 mM), and sucrose (10%) and separated on 12% Tricine gels (Schägger and von Jagow, 1987). Gels were stained with fluorescent Sypro Ruby (Molecular Probes, www.probes.invitrogen.com). 2D-IPG-SDS-PAGE protein separation was performed on the thylakoid soluble fraction using 150 μg of protein per IPG strip as previously described (Majeran et al., 2005). For 2D-BN-SDS-PAGE, equivalent amounts of WT and *hcf136* thylakoid membranes (700 μg of protein) were solubilized with n-dodecyl β-D-maltoside and separated in the native first dimension according to Schagger et al. (1994). Gel strips issued from the native dimension were reduced and alkylated in a solubilization buffer according to Majeran et al. (2005) and separated by second dimension SDS-Tricine 12% gels (Schägger and von Jagow, 1987). Gels were stained with Coomassie Brilliant Blue R-250 (USB Corporation, www.usbweb.com).

For protein identification, Coomassie Brilliant Blue or Sypro Ruby stained spots were picked manually. Spots were automatically washed and digested with modified trypsin (Promega) as previously described (Shevchenko et al., 1996), and peptides were extracted using a ProGest robot

(Genomic Solutions, www.genomicsolutions.com), dried and resuspended in 5% formic acid. Protein identification was performed by PMF using MALDI time-of-flight (TOF) MS in reflectron mode (Perseptive Biosystems Voyager DE-STR Workstation) and online LC-ESI-MS/MS (Micromass Q-TOF) according to Majeran et al. (2005). The MS or MS/MS spectra were searched against the maize EST assembly from TIGR (www.tigr.org) (ZmGI, v1.6) supplemented with maize chloroplast genome sequences obtained from NCBI (www.ncbi.nlm.nih.gov) using an in-house installation of Mascot (www.matrixscience.com).

Microarray

Total RNA was isolated from the second leaf of plants as described above. Six biological replicates were used to compare WT and mutant transcript profiles in separate M and BS experiments. To maximize biological replication, different seedling pools were used for each of the 12 hybridizations. Microarray experiments and analyses were performed according to Sawers et al. (2007) using the Maize Array Consortium oligonucleotide platform (www.maizearray.org). Feature intensity values were log-transformed and corrected for local background signal, and a LOWESS procedure (Dudoit et al., 2002) was used to normalize between channels. Features with either low or saturating signal intensity were discarded from further analysis. High expression filtering was less stringent to avoid elimination of previously characterized, high abundance, C_4 cell-specific transcripts. After filtering, features that were not assigned an MZ number by the Maize Array Consortium were discarded from further analysis. The moderated t-test (Smyth, 2004) using the R package limma was applied to

identify differentially expressed features. The p-values for each test (feature) were converted to q-values for false discovery rate analysis as described by Storey et al. (2004).

SYBR Green qPCR

Three biological replicates were used for qPCR, with two internal technical replicates for each reaction. Total RNA (8 µg) was treated with 3 U DNase I Amplification grade enzyme (Invitrogen) at 37°C for 30 min to remove contaminating DNA in the presence of 80 U RNaseOUT (Invitrogen). Enzymes and salts were removed from the RNA with TRIzol Reagents (Invitrogen). One µg purified RNA was incubated at 70°C for 10 min with 50 ng random hexamers and the reaction cooled on ice. Additional reagents were added to a final concentration of: 5 mM $MgCl_2$, 0.01M DTT, 0.5 mM dNTP, 40 U RNaseOUT and 200 U Superscript III RT (Invitrogen). Water was substituted for enzyme in the negative control. cDNA synthesis was performed by incubation at 25°C for 10 min, 50°C for 50 min, 80°C for 5 min and a 4°C soak. Upon completion, RNA template was destroyed with 2 U *E. coli* RNase H, and cDNA was diluted with 60 µl water. For qPCR reactions, template was further diluted with 3 parts water, and the SYBR Green JumpStart *Taq* ReadyMix without $MgCl_2$ kit (Sigma, www.sigma.com) was used with final concentrations of 2.3 mM $MgCl_2$ and 24 ng/µl forward and reverse primers. Primer sequences are available in Table 2.1. An internal reference dye was used to measure data quality. Samples were run at 95°C 2 min, cycled 47 times between 95°C 15 s and 60°C 1 min, followed by a dissociation stage of 95°C 15 s, 60°C 15 s and 95°C 15 s on an ABI Prism 7900HT Sequence Detection

System (Applied Biosystems). Data were analyzed using ABI Prism SDS 2.1 software. Results were normalized using 18S rRNA reactions as a control.

Accession numbers

Sequence data for the maize homologue of *Hcf136* can be found in the GenBank library under accession number EF587243. Full microarray data sets for M and BS cell experiments are available in MIAME compliant format in the Gene Expression Omnibus housed at the National Center for Biotechnical Information (www.ncbi.nlm.nih.gov/geo/). For Figure 2.1B, HCF136 homologues were aligned using the following accessions: *Z. mays* (ABQ53629), *Oryza sativa* (BAD62115.1), *A. thaliana* (O82660), *G. theta* (NP_113453.1) and *Synechocystis* sp. PCC 6803 (NP_440411). *Sorghum bicolor* protein information was assembled from CN132236, CN142773, CN142842, CN145337, CN150433, CN150507, and CN148500.

LITERATURE CITED

Andersen, K.S., Bain, J.M., Bishop, D.G., and Smillie, R.M. (1972). Photosystem II activity in agranal bundle sheath chloroplasts from *Zea mays*. Plant Physiol **49,** 461-466.

Barkan, A. (1988). Proteins encoded by a complex chloroplast transcription unit are each translated from both monocistronic and polycistronic mRNAs. EMBO J **7,** 2637-2644.

Barkan, A., Miles, D., and Taylor, W.C. (1986). Chloroplast gene expression in nuclear, photosynthetic mutants of maize. EMBO J **5,** 1421-1427.

Becker, T.W., Perro-Rechenmann, C., Suzuki, A., and Hirel, B. (1993). Subcellular and immunocytochemical localization of the enzymes involved in ammonia assimilation in mesophyll and bundle-sheath cells of maize leaves. Planta **191,** 129-136.

Brutnell, T.P., Sawers, R.J., Mant, A., and Langdale, J.A. (1999). BUNDLE SHEATH DEFECTIVE2, a novel protein required for post-translational regulation of the *rbcL* gene of maize. Plant Cell **11,** 849-864.

Burgener, M., Suter, M., Jones, S., and Brunold, C. (1998). Cysteine is the transport metabolite of assimilated sulfur from bundle-sheath to mesophyll cells in maize leaves. Plant Physiol **116,** 1315-1322.

Chollet, R. (1973). Photosynthetic carbon metabolism in isolated maize bundle sheath strands. Plant Physiol **51,** 787-792.

Cushman, J.C., Hallick, R.B., and Price, C.A. (1988). The two genes for the P700 chlorophyll a apoproteins on the *Euglena gracilis* chloroplast genome contain multiple introns. Curr Genet **13,** 159-171.

Dekker, J.P., and Boekema, E.J. (2005). Supramolecular organization of thylakoid membrane proteins in green plants. Biochim Biophys Acta **1706,** 12-39.

Dudoit, S., Yang, Y.H., Callow, M.J., and Speed, T.P. (2002). Statistical methods for identifying differentially expressed genes in replicated cDNA microarray experiments. Stat Sinica **12,** 111-139.

Edwards, G.E., and Walker, D. (1983). C_3, C_4: Mechanisms, cellular and environmental regulation of photosynthesis. (Berkeley: University of California Press).

Edwards, G.E., Furbank, R.T., Hatch, M.D., and Osmond, C.B. (2001a). What does it take to be C_4? Lessons from the evolution of C_4 photosynthesis. Plant Physiol **125,** 46-49.

Edwards, G.E., Franceschi, V.R., Ku, M.S., Voznesenskaya, E.V., Pyankov, V.I., and Andreo, C.S. (2001b). Compartmentation of photosynthesis in cells and tissues of C_4 plants. J Exp Bot **52,** 577-590.

Emanuelsson, O., Nielsen, H., Brunak, S., and von Heijne, G. (2000). Predicting subcellular localization of proteins based on their N-terminal amino acid sequence. J Mol Biol **300,** 1005-1016.

Friso, G., Giacomelli, L., Ytterberg, A.J., Peltier, J.B., Rudella, A., Sun, Q., and Wijk, K.J. (2004). In-depth analysis of the thylakoid membrane proteome of *Arabidopsis thaliana* chloroplasts: new proteins, new functions, and a plastid proteome database. Plant Cell **16,** 478-499.

Furumoto, T., Hata, S., and Izui, K. (2000). Isolation and characterization of cDNAs for differentially accumulated transcripts between mesophyll cells and bundle sheath strands of maize leaves. Plant Cell Physiol **41,** 1200-1209.

Ghirardi, M.L., and Melis, A. (1983). Localization of photosynthetic electron transport components in mesophyll and bundle sheath chloroplasts of *Zea mays*. Arch Biochem Biophys **224,** 19-28.

Gregory, R.P., Droppa, M., Horvath, G., and Evans, E.H. (1979). A comparison based on delayed light emission and fluorescence induction of intact chloroplasts isolated from mesophyll protoplasts and bundle-sheath cells of maize. Biochem J **180,** 253-256.

Harel, E., Lea, P.J., and Miflin, B.J. (1977). The localization of enzymes of nitrogen assimilation in maize leaves and their activities during greening. Planta **134,** 195-200.

Hibberd, J.M., and Quick, W.P. (2002). Characteristics of C_4 photosynthesis in stems and petioles of C_3 flowering plants. Nature **415,** 451-454.

Kagawa, T., and Hatch, M.D. (1974). C_4-acids as the source of carbon dioxide for Calvin cycle photosynthesis by bundle sheath cells of the C_4-pathway species *Atriplex spongiosa*. Biochem Biophys Res Commun **59,** 1326-1332.

Kim, J.K., and Hollingsworth, M.J. (1993). Splicing of group II introns in spinach chloroplasts (*in vivo*): analysis of lariat formation. Curr Genet **23,** 175-180.

Kirchanski, S.J. (1975). The ultrastructural development of the dimorphic plastids of *Zea mays* L. Amer J Bot **62,** 695–705.

Kolkman, J.M., Conrad, L.J., Farmer, P.R., Hardeman, K., Ahern, K.R., Lewis, P.E., Sawers, R.J., Lebejko, S., Chomet, P., and Brutnell, T.P. (2005). Distribution of *Activator* (*Ac*) throughout the maize genome for use in regional mutagenesis. Genetics **169,** 981-995.

Koussevitzky, S., Nott, A., Mockler, T.C., Hong, F., Sachetto-Martins, G., Surpin, M., Lim, J., Mittler, R., and Chory, J. (2007). Signals from chloroplasts converge to regulate nuclear gene expression. Science **316,** 715-719.

Ku, M.S., Kano-Murakami, Y., and Matsuoka, M. (1996). Evolution and expression of C_4 photosynthesis genes. Plant Physiol **111,** 949-957.

Kubicki, A., Steinmuller, K., and Westhoff, P. (1994). Differential transcription of plastome-encoded genes in the mesophyll and bundle-sheath chloroplasts of the monocotyledonous NADP-malic enzyme-type C_4 plants maize and sorghum. Plant Mol Biol **25,** 669-679.

Kuck, U. (1989). The intron of a plastid gene from a green alga contains an open reading frame for a reverse transcriptase-like enzyme. Mol Gen Genet **218,** 257-265.

Langdale, J.A., Rothermel, B.A., and Nelson, T. (1988a). Cellular pattern of photosynthetic gene expression in developing maize leaves. Genes Dev **2,** 106-115.

Langdale, J.A., Taylor, W.C., and Nelson, T. (1991). Cell-specific accumulation of maize *phosphoenolpyruvate carboxylase* is correlated with demethylation at a specific site greater than 3 kb upstream of the gene. Mol Gen Genet **225,** 49-55.

Langdale, J.A., Zelitch, I., Miller, E., and Nelson, T. (1988b). Cell position and light influence C_4 versus C_3 patterns of photosynthetic gene expression in maize. EMBO J **7,** 3643-3651.

Lee, M., Sharopova, N., Beavis, W.D., Grant, D., Katt, M., Blair, D., and Hallauer, A. (2002). Expanding the genetic map of maize with the intermated B73 x Mo17 (IBM) population. Plant Mol Biol **48,** 453-461.

Leto, K.J., and Miles, D. (1980). Characterization of three photosystem II mutants in *Zea mays* L. lacking a 32,000 Dalton lamellar polypeptide. Plant Physiol **66,** 18-24.

Majeran, W., Cai, Y., Sun, Q., and van Wijk, K.J. (2005). Functional differentiation of bundle sheath and mesophyll maize chloroplasts determined by comparative proteomics. Plant Cell **17,** 3111-3140.

Markelz, N.H., Costich, D.E., and Brutnell, T.P. (2003). Photomorphogenic responses in maize seedling development. Plant Physiol **133,** 1578-1591.

Maxwell, K., and Johnson, G.N. (2000). Chlorophyll fluorescence--a practical guide. J Exp Bot **51,** 659-668.

Meurer, J., Plucken, H., Kowallik, K.V., and Westhoff, P. (1998). A nuclear-encoded protein of prokaryotic origin is essential for the stability of photosystem II in *Arabidopsis thaliana*. EMBO J **17,** 5286-5297.

Miller, K.R., Miller, G.J., and McIntyre, K.R. (1977). Organization of the photosynthetic membrane in maize mesophyll and bundle sheath chloroplasts. Biochim Biophys Acta **459,** 145-156.

Plucken, H., Muller, B., Grohmann, D., Westhoff, P., and Eichacker, L.A. (2002). The HCF136 protein is essential for assembly of the photosystem II reaction center in *Arabidopsis thaliana*. FEBS Lett **532,** 85-90.

Rathnam, C.K., and Edwards, G.E. (1975). Intracellular localization of certain photosynthetic enzymes in bundle sheath cells of plants possessing the C_4 pathway of photosynthesis. Arch Biochem Biophys **171,** 214-225.

Rathnam, C.K., and Edwards, G.E. (1976). Distribution of nitrate-assimilating enzymes between mesophyll protoplasts and bundle sheath cells in leaves of three groups of C_4 plants. Plant Physiol **57,** 881-885.

Rock, C.D., Barkan, A., and Taylor, W.C. (1987). The maize plastid *psbB-psbF-petB-petD* gene cluster: spliced and unspliced *petB* and *petD* RNAs encode alternative products. Curr Genet **12,** 69-77.

Romanowska, E., Drozak, A., Pokorska, B., Shiell, B.J., and Michalski, W.P. (2006). Organization and activity of photosystems in the mesophyll and bundle sheath chloroplasts of maize. J Plant Physiol **163,** 607-618.

Roth, R., Hall, L.N., Brutnell, T.P., and Langdale, J.A. (1996). *bundle sheath defective2*, a mutation that disrupts the coordinated development of bundle sheath and mesophyll cells in the maize leaf. Plant Cell **8,** 915-927.

Sage, R.F. (2004). The evolution of C_4 photosynthesis. New Phytol **161,** 341-370.

Sawers, R.J., Liu, P., Anufrikova, K., Hwang, J.T., and Brutnell, T.P. (2007). A multi-treatment experimental system to examine photosynthetic differentiation in the maize leaf. BMC Genomics **8,** 12.

Schaffner, A.R., and Sheen, J. (1991). Maize *rbcS* promoter activity depends on sequence elements not found in dicot *rbcS* promoters. Plant Cell **3,** 997-1012.

Schaffner, A.R., and Sheen, J. (1992). Maize C_4 photosynthesis involves differential regulation of *phosphoenolpyruvate carboxylase* genes. Plant J **2,** 221-232.

Schagger, H., Cramer, W.A., and von Jagow, G. (1994). Analysis of molecular masses and oligomeric states of protein complexes by blue native electrophoresis and isolation of membrane protein complexes by two-dimensional native electrophoresis. Anal Biochem **217,** 220-230.

Schägger, H., and von Jagow, G. (1987). Tricine-sodium dodecyl sulfate-polyacrylamide gel electrophoresis for the separation of proteins in the range from 1 to 100 kDa. Anal Biochem **166,** 368-379.

Schuster, G., Ohad, I., Martineau, B., and Taylor, W.C. (1985). Differentiation and development of bundle sheath and mesophyll thylakoids in maize. Thylakoid polypeptide composition, phosphorylation, and organization of photosystem II. J Biol Chem **260,** 11866-11873.

Sheehan, M.J., Farmer, P.R., and Brutnell, T.P. (2004). Structure and expression of maize phytochrome family homeologs. Genetics **167,** 1395-1405.

Sheen, J. (1991). Molecular mechanisms underlying the differential expression of maize *pyruvate, orthophosphate dikinase* genes. Plant Cell **3,** 225-245.

Sheen, J. (1999). C_4 gene expression. Annu Rev Plant Physiol Plant Mol Biol **50,** 187-217.

Sheen, J., and Bogorad, L. (1986a). Expression of the *ribulose-1,5-bisphosphate carboxylase large subunit* gene and three small subunit genes in two cell types of maize leaves. EMBO J **5,** 3417-3422.

Sheen, J.Y., and Bogorad, L. (1986b). Differential expression of six light-harvesting chlorophyll a/b binding protein genes in maize leaf cell types. Proc Natl Acad Sci U S A **83,** 7811-7815.

Sheen, J.Y., and Bogorad, L. (1987). Differential expression of C_4 pathway genes in mesophyll and bundle sheath cells of greening maize leaves. J Biol Chem **262,** 11726-11730.

Shevchenko, A., Wilm, M., Vorm, O., and Mann, M. (1996). Mass spectrometric sequencing of proteins silver-stained polyacrylamide gels. Anal Chem **68,** 850-858.

Singh, M., Lewis, P.E., Hardeman, K., Bai, L., Rose, J.K., Mazourek, M., Chomet, P., and Brutnell, T.P. (2003). *Activator* mutagenesis of the *pink scutellum1/viviparous7* locus of maize. Plant Cell **15,** 874-884.

Smith, L.H., Langdale, J.A., and Chollet, R. (1998). A functional Calvin cycle is not indispensable for the light activation of C_4 phosphoenolpyruvate carboxylase kinase and its target enzyme in the maize mutant *bundle sheath defective2-mutable1*. Plant Physiol **118,** 191-197.

Smith, P.K., Krohn, R.I., Hermanson, G.T., Mallia, A.K., Gartner, F.H., Provenzano, M.D., Fujimoto, E.K., Goeke, N.M., Olson, B.J., and Klenk, D.C. (1985). Measurement of protein using bicinchoninic acid. Anal Biochem **150,** 76-85.

Smyth, G.K. (2004). Linear models and empirical bayes methods for assessing differential expression in microarray experiments. Stat Appl Genet Mol Biol **3,** Article3.

Stockhaus, J., Schlue, U., Koczor, M., Chitty, J.A., Taylor, W.C., and Westhoff, P. (1997). The promoter of the gene encoding the C_4 form of *phosphoenolpyruvate carboxylase* directs mesophyll-specific expression in transgenic C_4 *Flaveria* spp. Plant Cell **9,** 479-489.

Storey, J.D., Taylor, J.E., and Siegmund, D. (2004). Strong control, conservative point estimation and simultaneous conservative consistency of false discovery rates: A unified approach. J Roy Stat Soc B **66,** 187-205.

Strand, A., Asami, T., Alonso, J., Ecker, J.R., and Chory, J. (2003). Chloroplast to nucleus communication triggered by accumulation of Mg-protoporphyrinIX. Nature **421,** 79-83.

Susek, R.E., Ausubel, F.M., and Chory, J. (1993). Signal transduction mutants of *Arabidopsis* uncouple nuclear *CAB* and *RBCS* gene expression from chloroplast development. Cell **74,** 787-799.

CHAPTER THREE

FUNCTIONAL DISSECTION OF C_4 PHOTOSYNTHETIC DEVELOPMENT IN MAIZE USING CELL SPECIFIC BUNDLE SHEATH AND MESOPHYLL DEFECTIVE MUTANTS[*]

ABSTRACT

In *Zea mays*, photosynthetic activities are partitioned between two morphologically and biochemically distinct cell types, mesophyll (M) and bundle sheath (BS). These cells are organized in concentric rings around the vasculature and cooperate to fix carbon for photosynthesis. Partitioning of photosynthetic activities between M and BS cells is mediated by cell-specific localization of transcripts and proteins. However, regulation of this process is poorly understood. Here, we utilize two mutants selectively disrupted in M or BS cell development to assess the relative importance of sugar, energy metabolites and photosystem II (PSII) protein complex formation in establishing functional M and BS transcriptional networks. Comparative RNA transcript profiling was conducted between wild-type (WT) and a Rubisco-deficient mutant, *bundle sheath defective2* (*bsd2*). Transcriptomes from isolated M cells revealed very few differentially expressed features in the mutant, whereas many genes in BS cells accumulate to lower levels in *bsd2* relative to WT. These results suggest that M and BS transcriptomes are autonomously regulated by different signals.

[*] Microarray statistical analysis was performed by Prof. Peng Liu (Iowa State University). Fluorescence kinetics was measured by Prof. Thomas Owens (Cornell University).

INTRODUCTION

Maize, one of the world's most important food and biofuel crops, utilizes C_4 photosynthesis to fix carbon. The C_4 pathway in maize utilizes two morphologically and biochemically distinct cell types, mesophyll (M) and bundle sheath (BS). These cells develop as concentric files around the vasculature (Edwards and Walker, 1983) and photosynthetic activities are partitioned between them (Edwards et al., 2001; Majeran et al., 2005). M chloroplasts contain granal thylakoids, perform linear electron transport and photoreduce $NADP^+$ (Andersen et al., 1972). BS chloroplasts are agranal (Andersen et al., 1972; Kirchanski, 1975; Miller et al., 1977), lack functional photosystem II (PSII) (Schuster et al., 1985), generate ATP by cyclic electron transport and perform most Calvin cycle reactions (Chollet, 1973; Kagawa and Hatch, 1974). At least 1277 transcripts (Sawers et al., 2007) and 125 proteins (Majeran et al., 2005) differentially accumulate between M and BS cells.

How C_4 plants establish and maintain this complex morphology and biochemistry is poorly understood. It is generally believed that a developmental signal emanates from the vasculature, leading to C_4 photosynthetic differentiation (Langdale et al., 1988b; Langdale and Nelson, 1991). BS cells surrounding developing veins accumulate C_4 RNA expression patterns before Kranz anatomy is established, and M and BS cell differentiation is synchronized with vascular development (Langdale et al., 1987; Langdale et al., 1988a). Light is also required to initiate C_4 RNA and protein accumulation (Langdale et al., 1988b). In particular, an *Rbcs* enhancer element is induced by red/far-red light in BS cells and a repressor element is activated by blue light in M cells (Viret et al., 1994; Purcell et al., 1995). Other *cis*-regulatory elements are known to control expression of PEPC, RBCS, and

PPDK encoding genes (Langdale et al., 1991; Schaffner and Sheen, 1991; Sheen, 1991; Schaffner and Sheen, 1992; Stockhaus et al., 1997). Most recently, it has been hypothesized that the cellular environment, such as differences in sugar, redox, and protein complexes between cell types, plays a role in C_4 development (Sawers et al., 2007).

Here, we have performed a comparative analysis of M and BS transcript profiles from cell-specific mutants to characterize regulatory networks in C_4 development. The mutants *high chlorophyll fluorescence136* (*hcf136*) and *bundle sheath defective2* (*bsd2*) are specifically disrupted in M and BS plastid activities, respectively. *hcf136* lacks PSII (Chapter Two), and *bsd2* lacks Rubisco (Roth et al., 1996; Brutnell et al., 1999) and cannot perform Calvin cycle activities (Smith et al., 1998). Consequently, *hcf136* plastoquinone (PQ) pools are likely oxidized whereas *bsd2* PQ are reduced, and both mutants fail to accumulate sugars. As such, these mutants provide cellular perturbations useful for assessing the relative importance of redox, sugar, energy metabolites, and PSII protein complex accumulation in establishing M and BS transcript profiles.

Microarray analysis suggests that M and BS cells have autonomous transcriptional networks. M and BS transcript patterns are distinct when compared between cell types and between *bsd2* and *hcf136*, indicating the transcriptomes respond to different signals. Nuclear and plastid-encoded genes of the M cells may utilize unique plastid redox states and components or outputs of PSII complex formation to monitor plastid status. In contrast, nuclear and plastid genes of BS cells may respond to a signal that is disrupted in both the *hcf136* and *bsd2* mutants. A likely candidate signal is a sugar species that is not generated in the absence of a functional Calvin cycle.

RESULTS

bsd2 redox state is perturbed

Previous characterizations of *bsd2* have revealed a primary defect in Rubisco accumulation (Brutnell et al., 1999). However, the functionality of photosystem complexes in *bsd2* has not been reported. Quantum yield of PSII photochemistry was measured in the dark (Fv/Fm) and at three low actinic intensities ($Ø_{PSII}$; 5, 15, 35 μmol photons m^{-2} s^{-1}) in detached leaves from WT and *bsd2* seedlings (Figure 3.1). Quantum yield in WT declines only slightly over this light intensity range. In contrast, *bsd2* declines drastically, consistent with the loss of Rubisco in mutant tissue and the inability of the mutant to utilize ATP and NADPH produced by the light reactions (Roth et al., 1996; Smith et al., 1998). Note that the light intensities used to measure $Ø_{PSII}$ are far below the intensity required to saturate photosynthesis in WT maize. Thus, photosynthesis in *bsd2* saturates at very low light intensities.

We analyzed the contributions to lower quantum yield in *bsd2* by measuring photochemical quenching and the components of nonphotochemical quenching under the same light intensities as above (Figure 3.2). Consistent with the lack of electron acceptors in the mutant, photochemical quenching (qP) decreases more rapidly with increasing intensity relative to WT. The largest contribution to the decrease in quantum yield in *bsd2* is the increase in total nonphotochemical quenching (qN). The rapidly reversible component of qN, qE, is only slightly larger in *bsd2* than in WT, but the difference between qN and qE, photoinhibitory quenching (qI), is much larger in *bsd2* than in WT. These data demonstrate that low quantum yield in *bsd2* is largely due to qI in the mutant. However, the majority of qI appears to be due to the slowly relaxing component of qI since Fv/Fm

Figure 3.1. Photosystem II (PSII) quantum yield measured in the dark (Fv/Fm) and at low actinic illumination ($Ø_{PSII}$). Initial dark adaptation was for 60 minutes. Illumination at 5, 15, or 35 μmol was for six minutes at which time $Ø_{PSII}$ was measured.

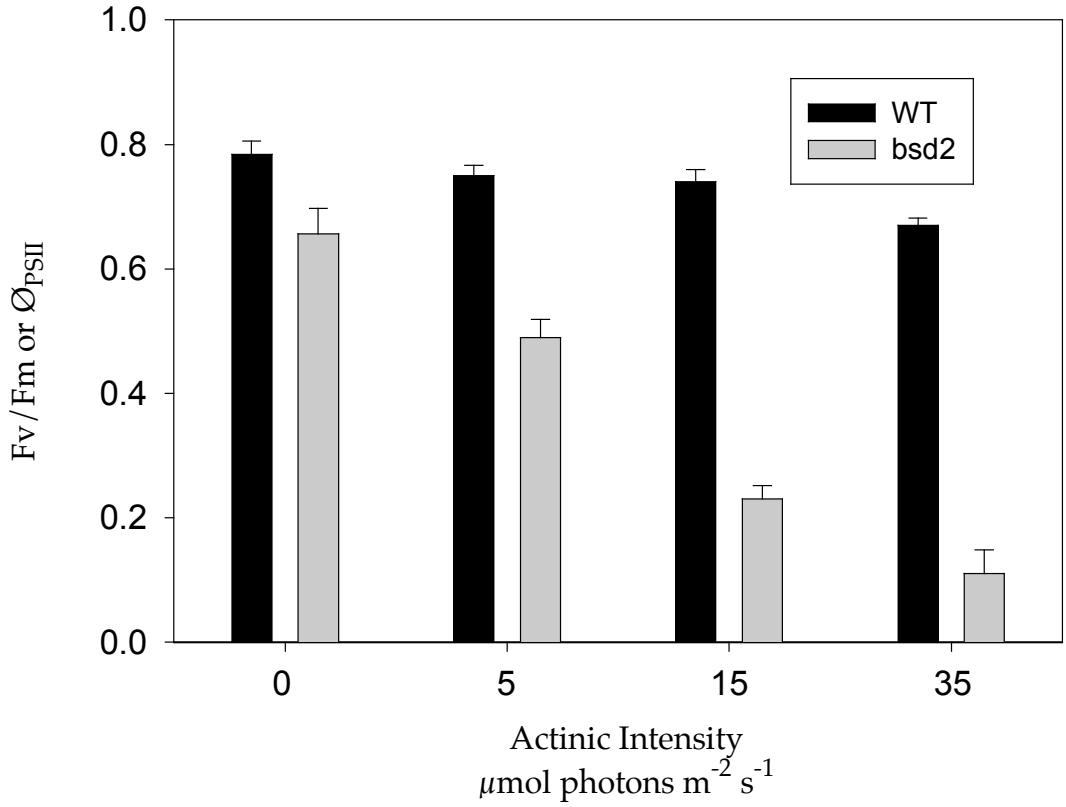
1.0
0.8
0.6
0.4
0.2
0.0
Fv/Fm or ØPSII
WT
bsd2
0
5
15
35
Actinic Intensity
μmol photons m-2 s-1

Figure 3.2. Measurements of photochemical quenching (qP), total nonphotochemical quenching (qN) and the rapidly reversible component of qN (qE) after six minutes of illumination at the indicated light intensities.

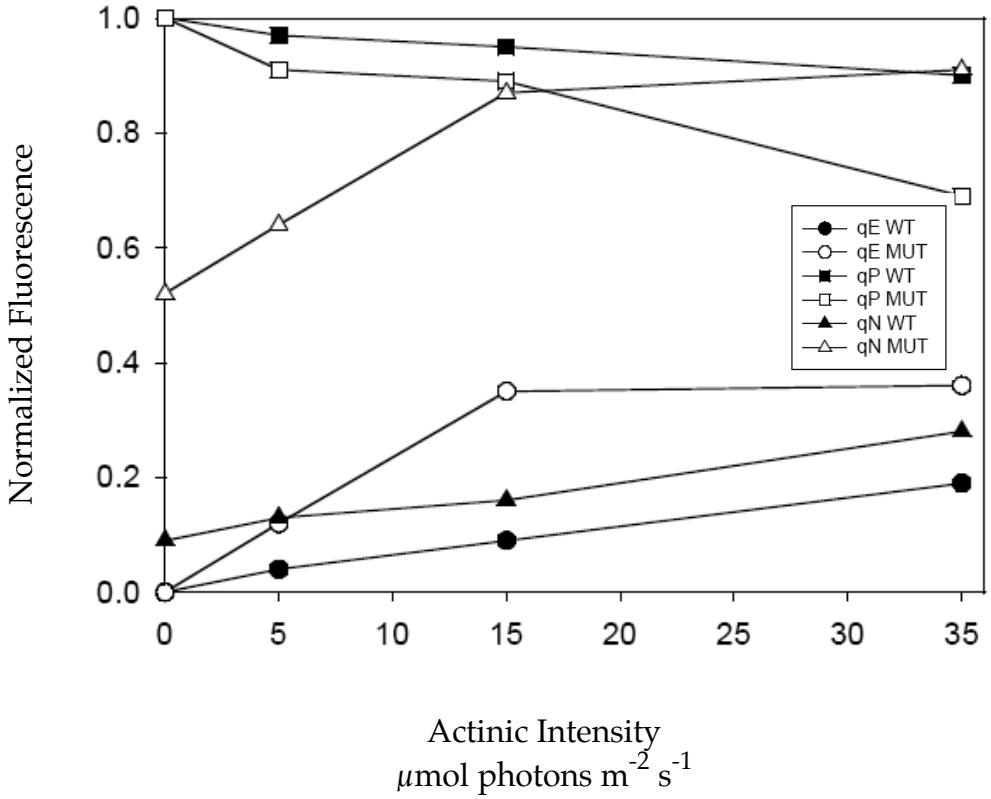
Normalized Fluorescence
1.0
0.8
0.6
0.4
0.2
0.0
0
5
10
15
20
25
30
35
qE WT
qE MUT
qP WT
qP MUT
qN WT
qN MUT
Actinic Intensity
μmol photons m-2 s-1

recovers in *bsd2* on the timescale of an hour (Figure 3.1).

To establish that the decrease in quantum yield is due to a photosynthetic component downstream of PSI, we measured the effects of far-red illumination on the kinetics of fluorescence recovery following a saturating pulse (Table 3.1). The fluorescence decay was fit to a sum of two exponentials $F(t)=A1\cdot e^{-b1\cdot t} + A2\cdot e^{-b2\cdot t}$. The data (Table 3.1) show that only the rate constant for the slower decay component (b2) is affected by far-red light and that the effect is the same in both WT and *bsd2*. Thus, PSI is functional in both WT and *bsd2* and the decrease in quantum yield must be attributed to some component of photosynthesis that is downstream of PSI.

Transcriptional profiling of separated BS and M cells

To examine the effects of the *bsd2* defect on gene expression, transcript profiles from isolated BS and M cells were examined using two-label microarray analysis. To avoid confounding treatment effects from the isolation of M protoplasts and BS strands (Sawers et al., 2007), dual label hybridizations were completed for six biological replicates for within cell type comparisons between WT and *bsd2* using the Maize Array Consortium platform (www.maizearray.org). After normalization and filtering, 4971 and 4126 features were considered for further analysis from the BS and M experiments, respectively. These two data sets share 3522 common features as summarized in Figure 3.3A.

Using a false discovery rate (FDR) of 5%, we identified 568 differentially expressed features in the comparison of *bsd2* and WT transcript BS cell profiles, of which 147 have at least a two-fold change in expression and 438 are less abundant in the mutant relative to WT. In the M cell comparison,

Table 3.1. Kinetic analysis of the decay of fluorescence following a 0.4 s saturating pulse of white light (4600 μmol photons m^{-2} s^{-1}). Decay was measured either in the dark (–FR; control) or in the presence of 45 μmol photons m^{-2} s^{-1} of 715 nm (+FR). Decays were fit to the sum of two exponentials with amplitudes A1 and A2 and rate constants of b1 and b2.

Light	A1		b1		A2		b2	
	WT	*bsd2*	WT	*bsd2*	WT	*bsd2*	WT	*bsd2*
-FR	0.73	0.69	4.1	4.3	0.27	0.31	0.16	0.11
+FR	0.67	0.63	3.9	4.4	0.33	0.37	0.27	0.24

Figure 3.3. Venn diagrams illustrating the degree of overlap between *bsd2* M and BS microarray data in (A) all detectable features and (B) features differentially expressed at a 5% false discovery rate (FDR).

A

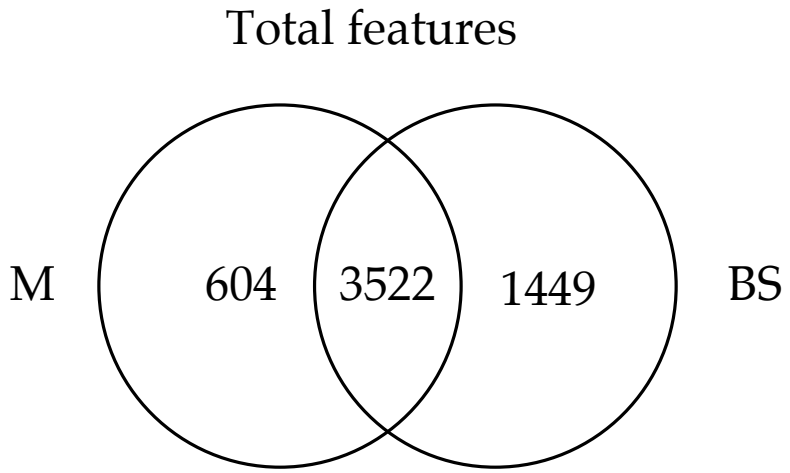

B

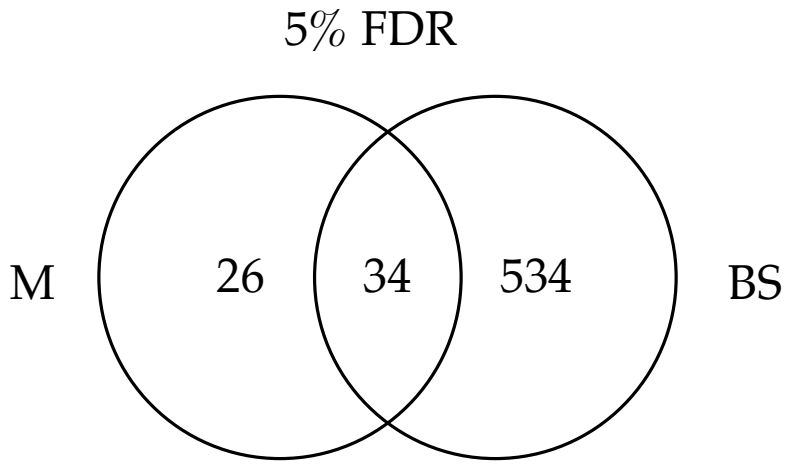

60 features are differentially expressed between *bsd2* and WT at a 5% FDR, of which seven have at least a two-fold change in expression and 35 are less abundant in the mutant relative to WT. When M and BS data sets are compared at a 5% FDR, 34 differentially expressed features are common to both cell types (Figure 3.3B). These data indicate that BS cells, where the primary lesion is located, have a much broader transcriptional response than M cells of the *bsd2* mutant.

Changes in plastid polycistronic processing cannot be directly assessed using the maize array platform. Therefore RNA blot analysis was used to test for such defects in separated *bsd2* M and BS cells (Figure 3.4). The *psbB-psbT-psbH-petB-petD* polycistron, which encodes components of both PSII and Cytochrome b_6f, was chosen for analysis because it is aberrantly processed in other photosynthetic mutants (Barkan et al., 1986) (Chapter Two). In *bsd2* M and BS cells, this polycistron shows normal processing relative to WT when hybridized with *psbH*. However, the relative abundance of some RNA species changes between mutant and WT. These data indicate that, unlike the *hcf136* mutant, we do not detect altered polycistronic processing in *bsd2*.

Validation of microarray data was performed by RNA blot analysis using probes designed to highly abundant transcripts that differentially accumulate relative to WT at 5% FDR in at least one cell type. As shown in Figure 3.5A and B, hybridization with nuclear-encoded *Lhcb-m7, Rbcs* and plastid-encoded *psaAB* and *rbcL* confirm differential accumulation of these transcripts in accordance with array results. For example, in the microarray analysis of M cells, detectable features representing *rbcL* (MZ00034482, MZ00034787, MZ00040486) are more abundant in *bsd2* relative to WT, consistent with previous results (Roth et al., 1996). In the BS cell microarray,

Figure 3.4. RNA blot analysis of isolated M and BS cells from *bsd2* and wild-type tissues shows no disruption to the processing of the plastid *psbB-psbT-psbH-petB-petD* polycistron when probed with *psbH*. Ethidium bromide (Etbr) staining of 18S rRNA after transfer to nitrocellulose membrane is shown as a loading control.

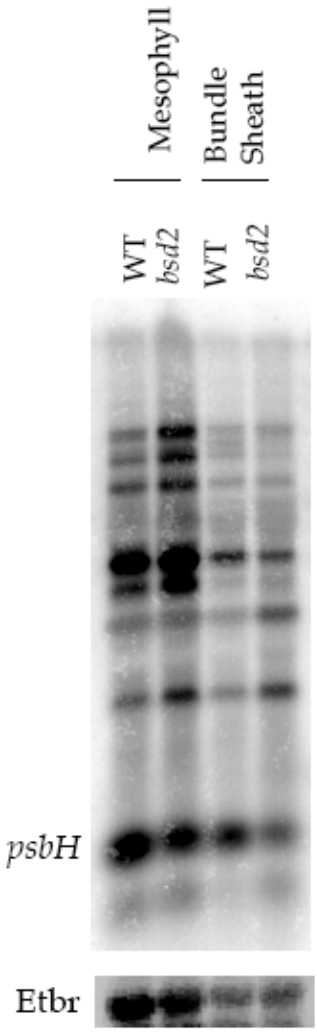
Mesophyll
Bundle Sheath
WT
bsd2
WT
bsd2
psbH
Etbr

Figure 3.5. RNA blot analysis of genes that are differentially expressed in at least one cell type according to *bsd2* M and BS microarray data. *Pepc* is shown as a loading control for panel A due to the ectopic expression of *rbcL* in this mutant. Ethidium bromide (Etbr) staining of 18S rRNA after transfer to nitrocellulose membrane is shown as a general loading control. Each panel (A and B) represents a successively probed blot loaded with separate biological replicates of RNA used in the microarray experiments. Hybridization with *rbcL, Lhcb, psaAB, Hcf136,* and *Rbcs* confirm the array data.

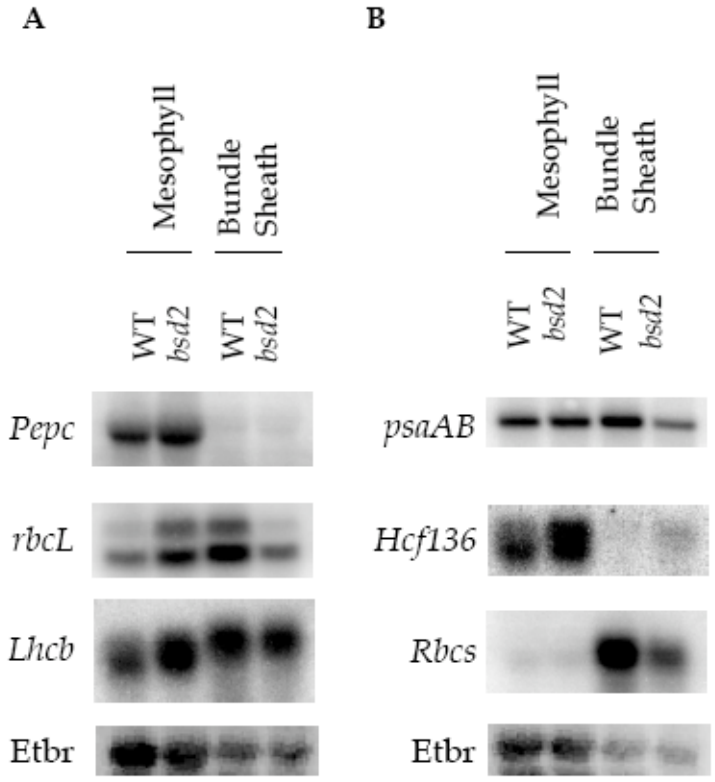
A
B
Mesophyll
Bundle Sheath
WT
bsd2
Pepc
rbcL
Lhcb
Etbr
psaAB
Hcf136
Rbcs
Etbr

the same *rbcL* features (MZ00034482, MZ00034787, MZ00040486) are 0.3, 0.4, and 0.4 fold less abundant than WT, respectively. FDR values are high for these features in M cells (14%, 19%, 42%, respectively) but are low in BS cells (0.1%, 1.6%, 0.8%, respectively). Hybridization with *Pepc*, an M cell specific marker, confirms the accuracy of the lanes. Verification analysis was also successful for *Hcf136*, a low abundance M cell-enriched transcript (Chapter Two) with an FDR value of 23% in the M cell experiment. Validation of increased *Hcf136* expression provides a positive marker against known data in *bsd2* total leaf tissue analysis (Figure 3.6). In addition, *rbcL* expression changes in the M and BS cells are consistent with previous reports (Roth et al., 1996). This confirmation analysis demonstrates that the array data accurately reflects transcriptional changes in *bsd2* M and BS cells.

Comparative analysis with WT spatial regulation

Data from *bsd2* BS and M cell experiments were compared against previously known WT C_4 BS:M ratios to identify features with atypical transcript accumulation (Sawers et al., 2007). When all data are controlled at 5% FDR, 25 BS-enriched features and 31 M-enriched features have altered BS:M ratios in *bsd2*. The direction of change, that is the increased or decreased differential expression between cell types, is dramatically different between these two classes. BS-enriched transcripts are less differentially expressed in *bsd2* (21/25), whereas M-enriched transcripts (29/31) are more differentially expressed relative to WT. For example, MZ00039735, a feature corresponding to glyceraldehyde-3-phosphate dehydrogenase, has a BS:M of 2.9 (Sawers et al. 2007), but in *bsd2* the predicted BS:M ratio is 1.1. Thus, this gene is less differentially expressed in the mutant. The trend for M- and BS-enriched

Figure 3.6. RNA blot analysis of *Hcf136* transcript levels in total leaf, bundle sheath, mesophyll, stressed total leaf, *hcf136* and *bsd2* total leaf tissues reveals that it is most abundant in *bsd2* (A). *Rbcs* and *Pepc* hybridization to the same RNA on a different blot show purity of the cell isolates (B). Ethidium bromide staining of 18S rRNA is shown as a loading control for both blots.

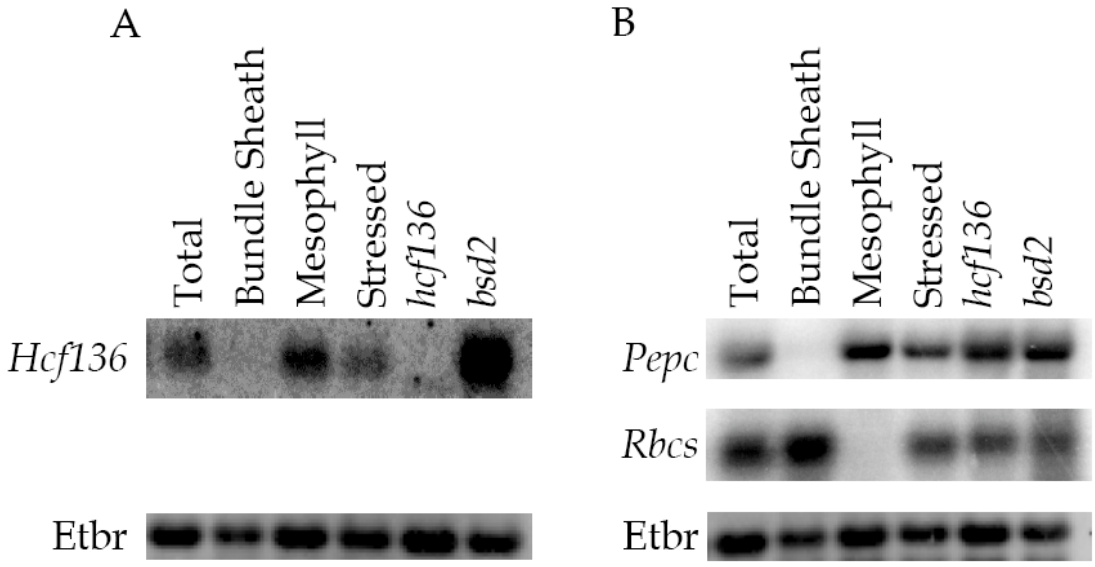
A
Total
Bundle Sheath
Mesophyll
Stressed
hcf136
bsd2
Hcf136
Etbr
B
Total
Bundle Sheath
Mesophyll
Stressed
hcf136
bsd2
Pepc
Rbcs
Etbr

transcripts is maintained even at a less stringent 15% FDR, which includes 162 BS-enriched and 229 M-enriched features. BS:M ratios decrease for 101 BS-enriched features and increases for 182 M-enriched features relative to WT. This comparison of WT and *bsd2* BS:M shows that BS- and M-enriched transcripts respond differently in a Rubisco deficient mutant.

Additionally, this comparative survey revealed dramatically altered patterns of expression for a few genes in the *bsd2* mutant. Transcripts corresponding to MZ00034483, MZ00027416, and MZ00011724 accumulate preferentially in the BS, with BS:M of 2.4, 2.2, and 3.3 respectively. However, in *bsd2* their predicted ratios are 0.7, 0.7, and 0.8, respectively, due to increased M cell transcript accumulation as well as decreased BS accumulation. Transcripts corresponding to MZ00023569 and MZ00023570 accumulate preferentially in M cells, with BS:M of 0.6 and 0.5, respectively. However, in *bsd2* their predicted ratios are 1.3 and 1.2 due to increased BS cell transcript accumulation. MZ00011724 and MZ00034483 encode unknown proteins. MZ00027416 is a putative MYB transcription factor. MZ00023569 encodes a putative protein translation factor, and MZ00023570 encodes a putative methylcrotonyl-CoA carboxylase. These data indicate that at least for some genes, it is possible to completely reverse the directionality of WT BS:M ratios.

DISCUSSION

bsd2 PQ pool is reduced

Consistent with its defect in Rubisco assembly (Roth et al., 1996), less light is necessary to reduce the PQ pool of *bsd2* than in WT. As observed in a series of actinic light measurements, *bsd2* has a reduced quantum yield, largely due to increased photoinhibition. Additionally, both *bsd2* and WT

exhibit similar fluorescence kinetics after exposure to far-red light, indicating that the decrease in quantum yield and increase in photoinhibition are due to a block downstream of PSI. Thus, it is likely that the lack of acceptors for NADPH due to loss of Calvin cycle activity (Smith et al., 1998) is leading to a more reduced PQ pool relative to WT.

M and BS cells have unique transcriptional networks

A comparison of basic patterns of expression between *bsd2* and *hcf136* mutants shows that the site of the primary lesion is most responsive to the disruption in photosynthetic activity. In *bsd2*, M cells contain very few differentially expressed features (60), suggesting this cell type does not have a large-scale genomic response to the loss of Rubisco in BS cells. This pattern is similar to M defective *hcf136*, in which BS cells have fewer differentially expressed features in response to the loss of PSII (2568 M versus 1669 BS; 5% FDR) (Chapter Two). However, in *bsd2*, 77% of differentially expressed features in BS cells are less abundant relative to WT, while in *hcf136*, 72% of features differentially expressed in M cells increase in abundance (Chapter Two). Lower transcript levels in *bsd2* BS cells account for BS:M expression changes for 75 of 101 BS-enriched features that are less differentially expressed between cell types as well as 169 of 182 M-enriched features that are more differentially expressed between cell types. Likewise, in *hcf136*, the general up-regulation of transcripts in M cells leads to most of the BS:M expression pattern changes in that mutant (Chapter Two). These data show that selectively disrupting M or BS cell development leads to a transcriptional response in both cell types, but BS and M cells respond uniquely to the perturbations in Calvin cycle activity and PSII, respectively.

M and BS transcriptional networks are mostly autonomous

BS and M cells share few differentially expressed features, and thus respond almost uniquely to the selective loss of Rubisco or PSII. Thus, the array data provides detailed evidence of autonomous but closely coordinated M and BS cell differentiation as previously suggested (Langdale et al., 1988a). In *bsd2*, 3522 features are detectable in both M and BS cells, and 34 overlapping features are differentially expressed at a 5% FDR. Similarly, 573 of 5670 shared features are differentially expressed in *hcf136* at a 5% FDR (Chapter Two). Thus, roughly 90% of the genes expressed in both BS and M cells respond uniquely to disruptions in PSII and Rubisco, indicating that independent transcriptional networks are operational in BS and M cells. This evidence for independent transcriptional control is in accordance with observations that WT BS cells can accumulate C_4 mRNAs before their neighboring M cells and that *argentia* mutants can establish C_4 specificity in the M cells first (Langdale et al., 1988a). Thus, M and BS cells behave relatively autonomously at the transcriptional level, even when perturbed.

Implications for C_4 development

Current models propose that the evolution of C_4 biology from the C_3 basal state relies on a plastic regulatory network (Muhaidat et al., 2007; Sawers et al., 2007). Given that 18% of the maize leaf transcriptome is differentially expressed between M and BS cells, a parsimonious explanation for development of C_4 metabolism is that only a few key regulatory changes are required and pathway integration relies on extant C_3 signaling networks. A corollary to this hypothesis is that in the absence of novel cellular environments, gene expression becomes less differential between cell types.

In support of this hypothesis, *Rbcs*, phosphoribulokinase, thioredoxin, and a 2Fe-2S iron sulfur cluster protein respond in both mutants with a decrease in BS:M expression. These data suggest that these transcripts are still operating under the control of extant C_3 signaling networks that are influenced by the cellular environment. In contrast, transcriptional control of *Carbonic anhydrase*, *Pepc*, *Ppdk*, *Me*, and *Mdh* may depend upon novel regulatory events that led to the establishment of C_4 photosynthesis as changes to their BS:M expression ratios are subtle and/or not altered in both mutant backgrounds.

METHODS

Plant growth conditions

Plants were grown in 16 h days, 50% humidity and a constant 28°C under low light conditions of 40 to 50 μmol/s^{-1}/m^{-2} for all experiments. Since *bsd2* is a lethal mutation, the line is maintained as a heterozygous stock, and experiments are performed on segregating homozygous mutants and their phenotypically wild–type siblings.

Fluorescence measurements

In vivo chlorophyll fluorescence parameters were measured by standard saturating pulse techniques (Maxwell and Johnson, 2000). All measurements were obtained at room temperature from the second leaf of seedlings at the third leaf emerging stage of development using an actinic light source and bright saturating pulse. Initial measurements of dark-adapted Fv/Fm were made after at least one hour in the dark. Leaves were then exposed to 5, 15, 35 μmol photons m^{-2} s^{-1} for six minutes at which time $Ø_{PSII}$

and the quenching parameters were measured. Samples were then dark adapted for 15 minutes to allow for relaxation of qE and measurement of qI (Melkonian et al., 2004).

For the far-red experiment, samples were dark adapted for at least 15 minutes. F_0 was measured and then samples were exposed to a 0.4 second saturating pulse of white light (4600 μmol m^{-2} s^{-1}) to close all reaction centers and establish F_m. The kinetics of the fluorescence decay back to F_0 in the dark was measured at 0.11 second intervals. Decay was measured either in the dark (control) or in the presence of 45 μmol photons m^{-2} s^{-1} of 715 nm far-red light (+/- 5 nm). Fluorescence was normalized between F_m=1 and F_0=0 and the decay was fit to a sum of two exponentials, $F(t)=A1\cdot e^{-b1\cdot t} + A2\cdot e^{-b2\cdot t}$. Decay rates were averaged from measurements of three different leaves. A modulated fluorescence apparatus was used for all experiments (model number FMS2) (Hansatech Instruments, Norfolk, UK).

Cell preparation

M protoplasts and BS strands were prepared as previously described (Chapter Two).

RNA isolation and blot analysis

Total RNA was isolated and analyzed by RNA blot as previously described (Sheehan et al., 2004). Leaf tissue was harvested at the third leaf emerging stage. Approximately, 15 μg of RNA was loaded for the confirmation of microarray analysis and studies of plastid polycistron processing. These RNA replicates are the same as those used in the microarray experiments. Ethidium bromide staining of the 18S rRNA on the nitrocellulose

blot was used a loading control. DNA probes for the RNA blot verification of microarray results include the nuclear-encoded *Pepc*, *Lhcb-m7*, *Hcf136*, and *Rbcs*. Plastid-encoded DNA probes include *psbH*, *rbcL* and *psaAB*. Primers used to create the probes are described in Chapter Two. Exposure times for these blots are 24 hours, with the exception of *psaAB* (3 hours), *rbcL* (3 hours), and *Hcf136* (multiple days). The RNA blot showing *Hcf136* expression in *bsd2* is loaded with 5 μg RNA and is a multiday exposure.

Microarray

Biological replicates were collected and the array protocol was performed as described in Chapter Two. Six biological replicates were used to compare WT versus *bsd2* mutant transcript profiles in distinct M and BS experiments. To maximize biological replication, different seedling pools were used for each of the 12 hybridizations. Labeling reactions were performed in a dye swap arrangement to control for differences in binding affinities of Cy3 and Cy5 probes and to maximize statistical reproducibility (Yang and Speed, 2002). After scanning, feature intensity values were log-transformed and corrected for local background. Features were filtered according to Chapter Two. The LOWESS procedure was used to normalize between channels for each slide. Following normalization, separate linear models including a gene-specific dye-effect (Smyth, 2004) was fit to the normalized log-scale data for each gene. A moderated-t test was then used to identify differentially expressed genes, and the resulting set of p-values was converted to q-values for FDR analysis as described by Storey and Tibshirani (2003). Along with q-values, fold-change estimates were calculated between *bsd2* and WT samples within cell type.

LITERATURE CITED

Andersen, K.S., Bain, J.M., Bishop, D.G., and Smillie, R.M. (1972). Photosystem II activity in agranal bundle sheath chloroplasts from *Zea mays*. Plant Physiol **49,** 461-466.

Barkan, A., Miles, D., and Taylor, W.C. (1986). Chloroplast gene expression in nuclear, photosynthetic mutants of maize. EMBO J **5,** 1421-1427.

Brutnell, T.P., Sawers, R.J., Mant, A., and Langdale, J.A. (1999). BUNDLE SHEATH DEFECTIVE2, a novel protein required for post-translational regulation of the *rbcL* gene of maize. Plant Cell **11,** 849-864.

Chollet, R. (1973). Photosynthetic carbon metabolism in isolated maize bundle sheath strands. Plant Physiol **51,** 787-792.

Edwards, G.E., and Walker, D. (1983). C_3, C_4: Mechanisms, cellular and environmental regulation of photosynthesis. (Berkeley: University of California Press).

Edwards, G.E., Franceschi, V.R., Ku, M.S., Voznesenskaya, E.V., Pyankov, V.I., and Andreo, C.S. (2001). Compartmentation of photosynthesis in cells and tissues of C_4 plants. J Exp Bot **52,** 577-590.

Hibberd, J.M., and Quick, W.P. (2002). Characteristics of C_4 photosynthesis in stems and petioles of C_3 flowering plants. Nature **415,** 451-454.

Kagawa, T., and Hatch, M.D. (1974). C_4-acids as the source of carbon dioxide for Calvin cycle photosynthesis by bundle sheath cells of the C_4-pathway species *Atriplex spongiosa*. Biochem Biophys Res Commun **59,** 1326-1332.

Kirchanski, S.J. (1975). The ultrastructural development of the dimorphic plastids of *Zea mays* L. Amer J Bot **62,** 695–705.

Langdale, J.A., and Nelson, T. (1991). Spatial regulation of photosynthetic development in C_4 plants. Trends Genet **7,** 191-196.

Langdale, J.A., Metzler, M.C., and Nelson, T. (1987). The *argentia* mutation delays normal development of photosynthetic cell-types in *Zea mays*. Dev Biol **122,** 243-255.

Langdale, J.A., Rothermel, B.A., and Nelson, T. (1988a). Cellular pattern of photosynthetic gene expression in developing maize leaves. Genes Dev **2,** 106-115.

Langdale, J.A., Taylor, W.C., and Nelson, T. (1991). Cell-specific accumulation of maize *phosphoenolpyruvate carboxylase* is correlated with demethylation at a specific site greater than 3 kb upstream of the gene. Mol Gen Genet **225,** 49-55.

Langdale, J.A., Zelitch, I., Miller, E., and Nelson, T. (1988b). Cell position and light influence C_4 versus C_3 patterns of photosynthetic gene expression in maize. EMBO J **7,** 3643-3651.

Majeran, W., Cai, Y., Sun, Q., and van Wijk, K.J. (2005). Functional differentiation of bundle sheath and mesophyll maize chloroplasts determined by comparative proteomics. Plant Cell **17,** 3111-3140.

Maxwell, K., and Johnson, G.N. (2000). Chlorophyll fluorescence--a practical guide. J Exp Bot **51,** 659-668.

Melkonian, J., Owens, T.G., and Wolfe, D.W. (2004). Gas exchange and co-regulation of photochemical and nonphotochemical quenching in bean during chilling at ambient and elevated carbon dioxide. Photosynth Res **79,** 71-82.

Miller, K.R., Miller, G.J., and McIntyre, K.R. (1977). Organization of the photosynthetic membrane in maize mesophyll and bundle sheath chloroplasts. Biochim Biophys Acta **459,** 145-156.

Muhaidat, R., Sage, R.F., and Dengler, N.G. (2007). Diversity of Kranz anatomy and biochemistry in C_4 eudicots. Amer J Bot **94,** 362-381.

Purcell, M., Mabrouk, Y.M., and Bogorad, L. (1995). Red/far-red and blue light-responsive regions of maize *rbcS-m3* are active in bundle sheath and mesophyll cells, respectively. Proc Natl Acad Sci U S A **92,** 11504-11508.

Roth, R., Hall, L.N., Brutnell, T.P., and Langdale, J.A. (1996). *bundle sheath defective2,* a mutation that disrupts the coordinated development of bundle sheath and mesophyll cells in the maize leaf. Plant Cell **8,** 915-927.

Sawers, R.J., Liu, P., Anufrikova, K., Hwang, J.T., and Brutnell, T.P. (2007). A multi-treatment experimental system to examine photosynthetic differentiation in the maize leaf. BMC Genomics **8,** 12.

Schaffner, A.R., and Sheen, J. (1991). Maize *rbcS* promoter activity depends on sequence elements not found in dicot *rbcS* promoters. Plant Cell **3,** 997-1012.

Schaffner, A.R., and Sheen, J. (1992). Maize C_4 photosynthesis involves differential regulation of *phosphoenolpyruvate carboxylase* genes. Plant J **2,** 221-232.

Schuster, G., Ohad, I., Martineau, B., and Taylor, W.C. (1985). Differentiation and development of bundle sheath and mesophyll thylakoids in maize. Thylakoid polypeptide composition, phosphorylation, and organization of photosystem II. J Biol Chem **260,** 11866-11873.

Sheehan, M.J., Farmer, P.R., and Brutnell, T.P. (2004). Structure and expression of maize phytochrome family homeologs. Genetics **167,** 1395-1405.

Sheen, J. (1991). Molecular mechanisms underlying the differential expression of maize *pyruvate, orthophosphate dikinase* genes. Plant Cell **3,** 225-245.

Smith, L.H., Langdale, J.A., and Chollet, R. (1998). A functional Calvin cycle is not indispensable for the light activation of C_4 phosphoenolpyruvate carboxylase kinase and its target enzyme in the maize mutant *bundle sheath defective2-mutable1*. Plant Physiol **118,** 191-197.

Smyth, G.K. (2004). Linear models and empirical bayes methods for assessing differential expression in microarray experiments. Stat Appl Genetic Mol Biol **3,** Article3.

Stockhaus, J., Schlue, U., Koczor, M., Chitty, J.A., Taylor, W.C., and Westhoff, P. (1997). The promoter of the gene encoding the C_4 form of *phosphoenolpyruvate carboxylase* directs mesophyll-specific expression in transgenic C_4 *Flaveria* spp. Plant Cell **9,** 479-489.

Storey, J.D., and Tibshirani, R. (2003). Statistical significance for genomewide studies. Proc Natl Acad Sci U S A **100,** 9440-9445.

Viret, J.F., Mabrouk, Y., and Bogorad, L. (1994). Transcriptional photoregulation of cell-type-preferred expression of maize *rbcS-m3*: 3' and 5' sequences are involved. Proc Natl Acad Sci U S A **91,** 8577-8581.

Yang, Y.H., and Speed, T. (2002). Design issues for cDNA microarray experiments. Nature reviews **3,** 579-588.

APPENDIX

AVAILABLE GERMPLASM

Genotype	Cross	Family
(*bsd2*) / + X (*l13*) / +	Self	SC07 – 1
(*bsd2*) / + X *cf1* / *cf1*	Self	SC07 – 2
(*bsd2*) / + X *tyd1* / *tyd1*; (*phyb1* / +)	Self	SC07 – 3
(*bsd2*) / + X *w2* / +	Self	SC07 – 4
elm1/*elm1* X *bsd2* / +	Self	SC07 – 6
elm1/*elm1* X *w3* / +	Self	SC07 – 7
l13 / + X *elm1*/*elm1*	Self	SC07 – 10
(*hcf136*) / + X *w3* / +	Self	SC07 – 12, 13
(*hcf136*) / + X *cf1* / *cf1*	Self	SC07 – 14
(*hcf136*) / + X *MZ3106* / +	Self	SC07 – 15
(*hcf136*) / + X *l13* / +	Self	SC07 – 16
B73 X *hcf136* / +	Self	SC07 – 18
T43 X *l13* / +	Self	SC07 – 19
T43 X *MZ3106* / +	Self	SC07 – 20
T43 X *oro1* / +; *elm1* / +	Self	SC07 – 21 SC06 – 31
T43 X *w1* / +	Self	SC07 – 22
T43 X *w3* / +	Self	SC07 – 23
T43 X *l19* / +	Self	SC07 – 24
T43 X *cf1* / *cf1*	Self	SC07 – 25
T43 X (*oy700*) / +; (*elm1*) / +; *oro* / +	Self	SC07 – 26

Genotype	Cross	Family
T43 X *oro1* / +	Self	SC07 – 27
T43 X *tyd1* / *tyd1*	Introgress	SC07 – 69
T43 X *oy1989* [W22 5?] / +	Introgress	SC07 – 37, TK07 – 15 KA07 – 71
bsd2 / + X *hcf136* / +	Self	SC06 – 13, 14
bsd2 / + X *tyd1*/*tyd1*		SC06 – 50
w3 / +; *oy1989* / +; (*elm1*) / +	Self	SC07 – 28
*l**N1836 / +	Self	SC06 – 83
bsd2 / +; *hcf136* / +	Self	SC06 – 111 SC06 – 112